Mechanical Systems and Signal Processing 230 (2025) 112587

Contents lists available at ScienceDirect

Mechanical Systems and Signal Processing

journal homepage: www.elsevier.com/locate/ymssp

On-board identification of wheel polygonization of metro trains based on convolutional neural network regression analysis and angular-domain synchronous averaging

Wenjing Sun [a,b,*], Xuan Geng [b], David J. Thompson [a], Tengfei Wang [b], Jinsong Zhou [b], Jin Zhang [c]

[a] Institute of Sound and Vibration Research, University of Southampton, Southampton SO17 1BJ, United Kingdom
[b] Institute of Rail Transit, Tongji University, Shanghai 201804, PR China
[c] Zhejiang Lab, Hangzhou 311100, PR China

ARTICLE INFO

Keywords:
Rail vehicle
Wheel polygonization level
Axle box acceleration (ABA)
Angular-domain synchronous averaging (ADSA)
Convolutional neural network (CNN)

ABSTRACT

Wheel polygonization, a form of wheel out-of-roundness, has become a common problem on trains of urban rail transit systems in recent years. It results in a significant increase of the dynamic responses of both the vehicle and the track, high vibration and noise levels, and structural fatigue. This paper proposes an innovative method for identifying wheel polygonization orders and their effective values using convolutional neural network (CNN) regression analysis. First, the acceleration signal measured on the axle box has been processed with the angular-domain synchronous averaging (ADSA) method, effectively separating the characteristic information associated with wheel polygonization within the signal. To extract comprehensive wheel polygonization information, a feature fusion method is employed, integrating features from both the time and frequency domain. Then, a CNN regression model is established and trained, with validation conducted using measured data of vehicle vibration and the wheel polygonization measured during field tests. Comparative analysis with different identification methods is performed, including a comparison of different preprocessing methods and machine learning models, which demonstrates the effectiveness of the proposed method in this study. The verification results show that the proposed method achieves high identification accuracy for wheel polygonization up to the 25th order. The overall average root mean square error value is 2.0 dB. Finally, the influence of wheel polygonization conditions, track stiffness, and speed fluctuation on the identification accuracy is discussed. The results show the proposed method exhibits robust identification capacity under varying conditions, which indicates its wide application and accuracy in complex situations during train service. This research contributes to advancing the field of wheel polygonization detection, offering a reliable and effective solution for application in railway systems.

1. Introduction

Wheel polygonization is a common form of wheel out-of-roundness (OOR), which is mainly manifest as a periodic deviation of

* Corresponding author.
E-mail address: w.sun@soton.ac.uk (W. Sun).

https://doi.org/10.1016/j.ymssp.2025.112587
Received 17 February 2024; Received in revised form 29 January 2025; Accepted 13 March 2025
Available online 19 March 2025

wheel radius around the circumferential direction [1]. In recent years, wheel polygonization has become a common problem on trains of urban rail transit systems, resulting in a significant increase of the dynamic responses of both the vehicle and the track components [2], abnormal vibration and noise of rail vehicles, and structural fatigue [3]. Chen et al. [4] found the wheel polygonization of orders 1–25 has the greatest impact on the operation of the vehicle. The wheel polygonization below the 4th order has a great impact on the running comfort of the train, while the higher orders above the 10th have a great impact on structural fatigue and noise [5]. Zhang et al. [6] studied the influence of wheel polygonization on noise levels in high-speed trains, and found the interior noise increased by 8–10 dB in the frequency range 200–2000 Hz in the presence of polygonization.

In addition, due to the significant increase in the wheel/rail interaction force caused by the wheel polygonization [7], fatigue fracture of key components of the vehicle, such as coil springs [8] and axles [9], may occur, shortening the life of the wheel-rail system [10,11]. Therefore, it is necessary to detect and maintain the state of the wheels regularly to ensure the running safety and ride quality of the train during operation. Reprofiling is the main measure available to mitigate the polygonization of wheels. However, in some cases, the wheel after reprofiling may also have residual polygonization or imperfect reprofiling, so it is important to identify the wheel condition to confirm whether the wheel meets the requirements.

Current detection methods for wheel polygonization can mainly be divided into two kinds: direct and indirect methods. The direct method refers to the measurement of the wheels manually with relevant equipment during train maintenance. The test results of this method are relatively accurate, but the vehicle needs to be out of service, and factors such as operating time and human factors result in high cost and low efficiency. The indirect methods identify the OOR state of the wheels through the dynamic responses of the vehicle-track coupled system, such as vibration signals [12], noise signals [13,14] etc., which has the advantages of convenience, high efficiency and low cost. Currently, a significant amount of research [15–18] focuses mainly on qualitative detection and identification of a certain level of wheel out of roundness under abnormal wear conditions. Xu et al. [19] addressed early wheel polygonal wear detection and disturbance suppression using the WASMA (weighted angle-synchronous moving average) filter, which effectively filters out typical disturbances to reduce the misdiagnosis of early wheel polygonization. However, precise identification of multiple orders of wheel polygonization and their amplitudes has yet to be achieved.

The studies of Yang et al. [20] and Wu et al. [21] showed that the safety of vehicle operation can be reflected through the acceleration of the axle box. Wu et al. [22] verified the correlation between axle box acceleration (ABA) and OOR through tests and clarified the feasibility of dynamic monitoring of the wheel OOR based on the ABA. Most of the traditional signal processing methods based on monitoring wheel OOR using ABA are used at present, starting from the perspective of time–frequency analysis. Wang [23] proposed an improved Wigner-Ville method, which can infer whether the type of wheel OOR belongs to the wheel polygonization according to the vibration acceleration. Li et al. [24] used a time-domain index analysis to identify wheel flats and estimate their severity. Wang et al. [25] proposed a method for identifying wheel OOR based on sparse track irregularity data and adopted a dense sampling algorithm to identify the main vibration frequency related to the wheel polygonization. At the same time, it was pointed out that, due to the influence of the track irregularity excitation, it is necessary to combine the relevant processing methods to separate the response due to rail and wheel excitation. In response to this problem, Chen et al. [26] proposed a wheel polygonization detection method based on adaptive chirp mode decomposition (ACMD), which can separate the wheel polygonization feature signal. An improved frequency domain integration method was developed by Xie et al. [27] to quantitatively capture the orders and the roughness levels of wheel polygonization. Carrigan and Talbot [28] proposed a method to identify the wheel OOR from the combined roughness signal obtained from ABA by means of circular averaging. They then proposed a new method to derive the rail roughness from ABA as well [29]. The above indirect detection methods have improved efficiency compared with direct measurement, but generally only the polygonization orders with the highest levels and their effective values are detected, and the overall accuracy for multiple orders of wheel polygonization still needs to be studied and further improved.

With the dramatic increase in computing capacity, neural networks and deep learning have become widely used. The convolutional neural network (CNN) has great advantages in dealing with nonlinear problems and can effectively analyze the nonlinear relationship between the vibration of the axle box and the wheel/rail excitation. The application of neural networks in wheel polygonization detection primarily involves classification and regression problems. The existing research mostly focuses on classification tasks, mainly used to distinguish damage caused by out-of-round wheels. For instance, Shi et al. [30] proposed a lightweight CNN that utilized vehicle body acceleration to detect the presence of out-of-round wheels, achieving an identification accuracy of 98 %. Deng et al. [31] employed a one-dimensional CNN to recognize the types of wheel damage, such as polygonization and scratches, achieving a recognition accuracy of 99 %. Xie et al. [32] proposed a model based on an optimized multiple kernel extreme learning machine, which can only effectively extract the main order of polygonal wheels from axle box acceleration. For the regression problem of identifying the amplitude of different wheel orders of various wavelengths, Ye et al. [33] employed a CNN for recognition. The root mean square error (RMSE) of the first 25 orders was approximately 5.8 dB. However, this approach was solely based on simulated data and proved to be highly sensitive to variations in train speed. Dong et al. [34] proposed a quantitative detection method for wheel OOR using a hybrid deep learning model (CNN-LSTM) for heavy-haul locomotives. While effective in identifying dominant orders of wheel polygonization and their amplitudes for heavy-haul locomotives, the CNN-LSTM model is more complex than a standalone CNN model, requiring longer processing time for polygonization identification.

In summary, previous studies have shown that the ABA signal contains relevant information related with wheel polygonization. Using ABA signals for wheel polygonization detection is a very efficient indirect measured method. However, due to interference factors such as rail roughness, track stiffness and speed fluctuations, the detection accuracy is insufficient, and the identification of wheel polygonization conditions is still mostly limited to the prominent order and its severity rather than multiple orders of wheel polygonization. Additionally, some studies, e.g. [35,36], only used simulated data for analysis and validation, without any practical application on data from actual vehicle operation. The application of neural network methods has been combined with the traditional

signal processing methods to improve the identification accuracy. However, the existing approaches still mostly adopt a classification method to distinguish the severity of wheel polygonization rather than analyze it quantitatively. The method of combining neural networks with regression analysis can allow quantitative analysis of the amplitude of each order of wheel polygonization but requires a large amount of training data and an appropriate network structure. There are several issues that need to be addressed in the current research on using neural network regression analysis: (1) Models are very sensitive to vehicle speed, and subtle changes in vehicle speed can cause significant errors; (2) If the training data and validation data are both simulated data this cannot determine their effectiveness in practical applications. Overall, there is a need for further research in integrating regression methods and addressing the aforementioned issues in order to achieve more robust and accurate recognition of non-round wheels.

Compared with previous research, the method proposed in this paper combines several key features: (1) The proposed method, combining CNN and ADSA aims to simultaneously identify the specific amplitudes of wheel polygonization with multiple different orders and wavelengths with high accuracy. (2) The method has been tested for both mild and severe polygonization levels. (3) It is designed to mitigate the influence of various factors, including track properties and train speed, specifically addressing the challenges posed by variations in track stiffness, thereby enhancing its reliability and practical applicability. (4) Measured data from field tests of different metro vehicles has been used for validation, ensuring the generality and effectiveness of this indirect approach based on ABA signals. The rest of the paper is organized as follows: Section 2 introduces field measurements that are used to provide input data. Section 3 then describes the framework of the proposed wheel polygonization detection method. The angular-domain synchronous averaging (ADSA) method is first employed to separate the wheel polygonization characteristic signal from the ABA signals. Then the pre-processed signals are taken into the CNN to identify the orders and the effective values of wheel polygonization. A vehicle-track coupled dynamic model is established and verified with measured data. It is then used to generate a large number of samples for CNN training in Section 4. Subsequently, the establishment of both the CNN and the sample dataset are described. In Section 5, the results obtained for the first 25 orders of polygonization are identified from on-board measurements on urban rail vehicles and the overall accuracy is determined from field tests. The accuracy of the proposed method is compared with results from alternative methods. The influence of several factors on the identification results, such as the severity of polygonization, and variations in track stiffness and train speed, is also discussed in this section. The main conclusions are summarized in Section 6.

2. Field tests

To provide input data for simulations used in training the CNN and to verify the accuracy and applicability of the proposed method of wheel polygonization identification, the OOR of multiple wheels of different trains and corresponding ABA data are both needed. EN 15610 [37] describes the measurement and data processing procedure for wheel and rail roughness. The rms value can be used to quantify the roughness of the wheel surface in a given wavelength band. The roughness level L_w of the wheel is defined as follows:

$$L_w = 10\log_{10}\left(\frac{r_{rms}}{r_0}\right)^2 \tag{1}$$

where L_w is the wheel surface roughness level in dB; r_{rms} is the rms value of the wheel surface roughness amplitude (in a given wavelength band); and r_0 is the reference value, 1×10^{-6} m.

The wheel OOR measurements were carried out manually with the direct method as shown in Fig. 1(a), which are time consuming. The wheel was lifted clear of the rail and measured with the M Wheel instrument, attached to the rail surface with the sensor in contact

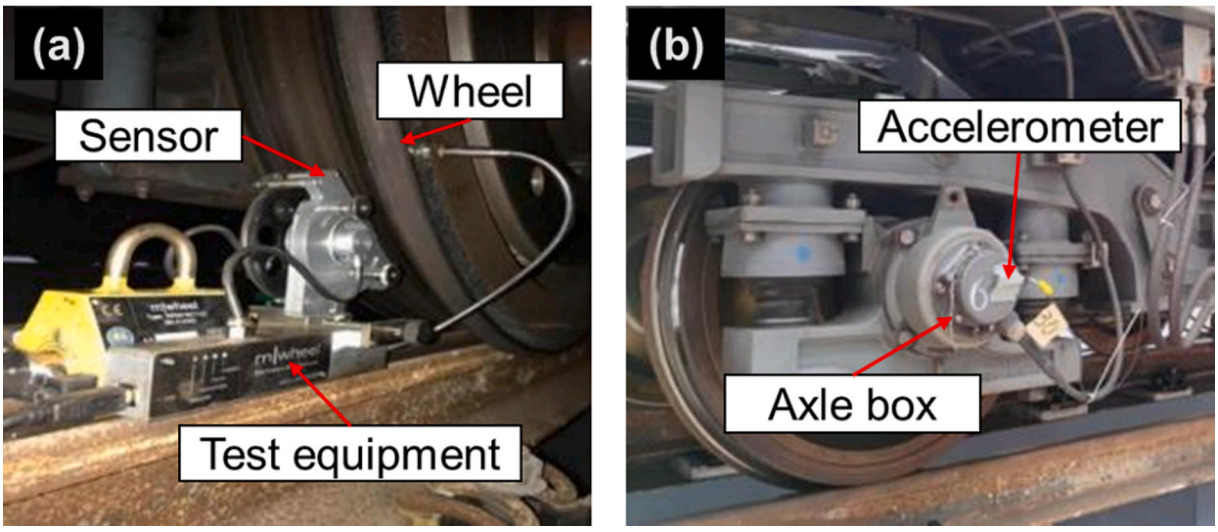

Fig. 1. Field tests. (a) Wheel OOR measurement; (b) ABA measurement.

the wheel tread surface. The OOR of the wheel can be measured by rotating the wheel several times. The ABA response of vehicles was also measured, which has been used first to validate the vehicle-track coupled dynamic model and second to verify the accuracy of the proposed method of OOR identification. The ABA measurements were made on two wheels each of two trains, corresponding with the ABA response before and after re-profiling, which are used to verify the identification results later. The accelerometer on the axle box was installed as shown in Fig. 1(b). At the same time, the speed of the train was recorded.

Some example measurement results of the wheel circumferential profile obtained from the field tests are shown in Fig. 2. These wheels have different degrees of OOR condition.

Fig. 3 shows examples of the measured ABAs before and after re-profiling of the wheel. The degree of the wheel polygonization has a great influence on the ABA response.

As an important part of the track system, the stiffness of the track fastener also has a significant impact on the vibration of both vehicle and track system. For the same train running on track sections with different fasteners, the ABA test results are shown in Fig. 4. The ABA signals are very different for different track sections due to the differences of the track conditions, including the rail pad stiffness and the track irregularity or rail roughness. It can also be observed that, as the running speed of the train increases as it departs from a station and decreases as it approaches the next one, the ABA signal is strongly affected.The above test results show that the ABA can reflect the severity of the wheel polygonization, which is why it is selected as the indirect measurement of the polygonization degree of the wheel. At the same time, however, there are many uncertainties that affect the ABA, such as the stiffness of the track fastener, the speed of the vehicle, the rail roughness, etc. Due to this, it has proved very difficult in previous studies based on numerical models or traditional signal processing methods to achieve precise identification of the level of each wheel polygonal order. Whether the wheel polygonization can be quantified under complex conditions using the proposed method is the key question to be answered. In this paper, the CNN method is proposed to increase the identification accuracy in the presence of different kinds of uncertainties in practical operational environments.

3. Framework of wheel polygonization identification method

3.1. CNN model

CNN are increasingly applied in image recognition [38], fault diagnosis [39], etc. The main structure of CNN includes an input layer, a hidden layer, and an output layer. Of these, the hidden layer is the most important part of the CNN and is mainly composed of multiple alternating convolution layers and pooling layers. In order to speed up the training and convergence of the neural network, to control the gradient explosion and to prevent overfitting [40], a batch normalization (BN) layer is added after each convolution layer. At the same time, the rectified linear unit (ReLU) activation function is adopted after the BN layer. The formula [41] describing the ReLU activation function f is as follows:

$$f(g(i)) = max\{0, g(i)\}, i = 1, 2, \cdots, n \tag{2}$$

where $g(i)$ is the output value of the i-th layer and also the input value of the function ReLU, n is the network layer number.

This constitutes a Convolution-Batch Normalization-ReLU (Conv-BN-ReLU or CBR) module. The CBR module and pooling layer alternate to form the basic structure of the proposed CNN, as shown in Fig. 5.

There are multiple convolution kernels in the convolution layer, and their main function is to convolve the input data with the convolution kernel to extract the feature information in the data. The process of the convolutional layers [42] is shown as follows:

$$g(i) = k_i^j * g(i-1) + b_i^j \tag{3}$$

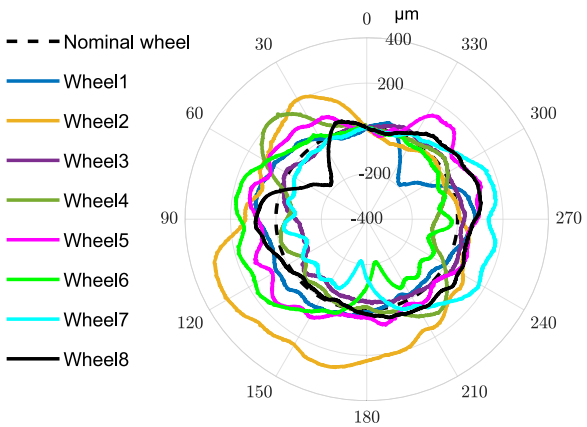

Fig. 2. Examples of some wheel profiles.

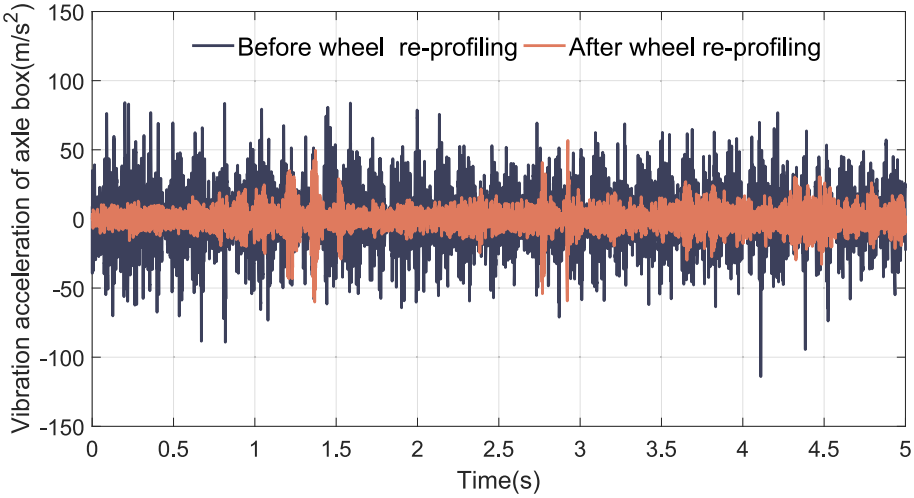

Fig. 3. Comparison of ABA signals before and after wheel re-profiling.

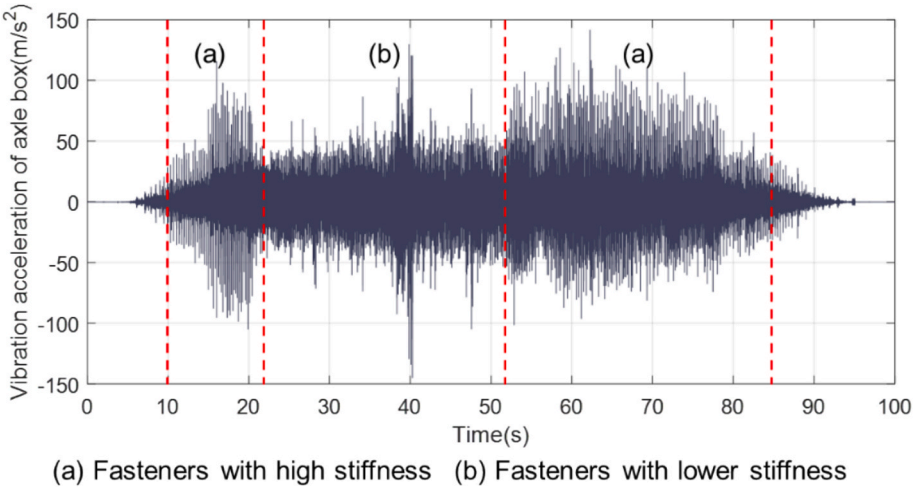

Fig. 4. Comparison of ABA signals of train running on track sections with different fasteners.

where * represents convolution operation, $g(i)$ represents the output data of the i-th layer, k_i^j represents the i-th convolution kernel of the j-th layer, b_i^j is the corresponding bias.

The pooling layer applies the pooling kernel to obtain a sub-sample of the input data to extract features while reducing the data dimensionality [43]. There are two common types of pooling layer: maximum pooling and average pooling. Of these, maximum pooling has the best effect and is widely used. Its formula is as follows [44]:

$$p^{l(i,j)} = max_{(j-1)w<t<jw}\left\{a^{l(i,t)}\right\}, j = 1, 2, \cdots, nl \tag{4}$$

where $a^{l(i,t)}$ represents the t-th neuron of the i-th map in the l-th layer. w represents the width of the convolution kernel, and j represents the j-th pooling kernel.

3.2. Regression analysis and multi-modal fusion

Regression analysis is a statistical analysis method that can analyze and determine the quantitative relationship between variables [45]. If there is a relationship between the independent variable $x_1, x_2, \cdots x_n$ and the dependent variable y, then when the independent variable takes a certain value, the dependent variable has a corresponding probability distribution, and the probability model between variables can be expressed as [46]:

$$y = r(x_1, x_2, \cdots x_n) + \varepsilon \tag{5}$$

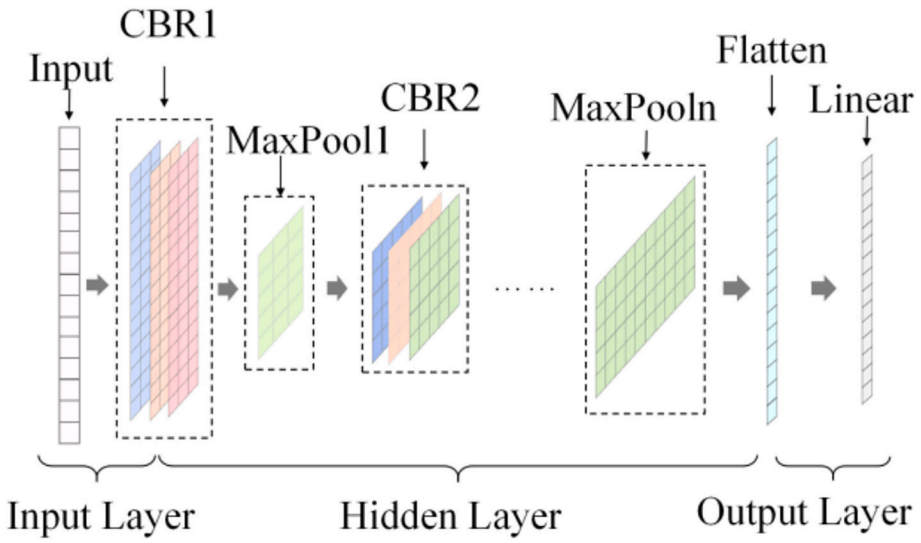

Fig. 5. Schematic diagram of proposed CNN.

where y represents the dependent variable, $x_1, x_2, \cdots x_n$ represents the independent variables, $r(x_1, x_2, \cdots x_n)$ represents the mapping relationship between the independent variables and the dependent variable, and ε represents the error. The relationship between neural networks and regression analysis [47] is shown in Fig. 6.

Regression analysis allows the relationship between the wheel polygonization and the ABA to be established, and the mapping relationship between them to be obtained; this can be used to detect the wheel polygonization state from the ABA signal. Since the relationship between the polygonization of the wheel and the ABA is nonlinear and complex, it is difficult to calculate this relationship, and it is also impossible to express the relationship between the variables in a concise mathematical model. However, the neural network has significant advantages in analyzing nonlinear problems. Therefore, the combination of regression analysis and neural network can fully consider the nonlinear relationship between both the order and the level of the wheel polygonization and the dynamic response of the axle box, to achieve a correct identification result.

The same object can be described by different features. The process of combining multiple features for deep learning tasks is called feature fusion, also known as multi-modal fusion technology (MFT) [48]. This method integrates different types of feature data as the input of the network, thereby improving the detection accuracy of the neural network model.

The measured ABA signals are typically obtained as discrete time series. Extracting information about signal variations over time can be achieved from the time-domain signal, while Fourier transformation enables the acquisition of amplitude information at different frequencies. The information derived from both the time and frequency domains is mutually complementary. Therefore, by integrating these two types of data, a more comprehensive analysis of the impact of wheel polygonization on the ABA can be

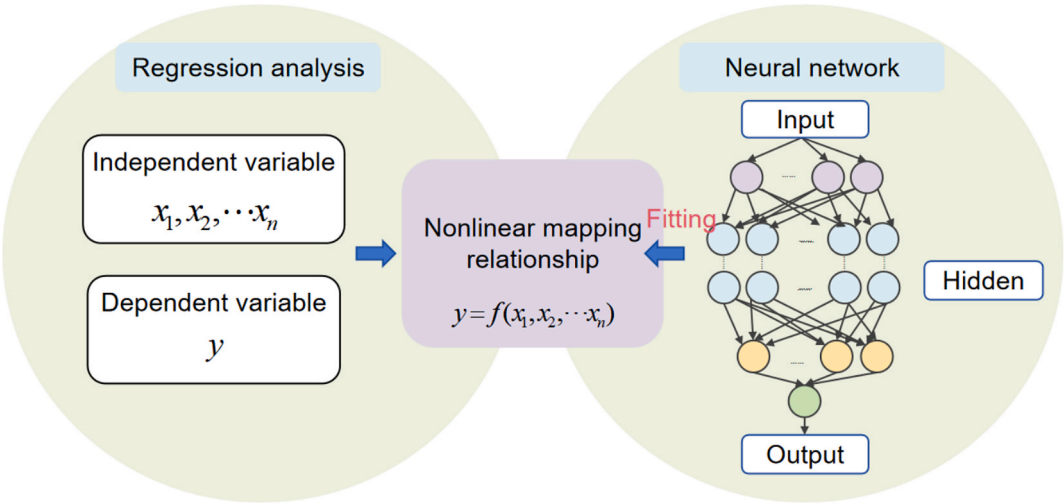

Fig. 6. Regression analysis and neural networks.

conducted, leading to a more accurate deduction of the amplitude levels for each wheel polygonization order.

In this study, a synergistic approach of regression analysis and convolutional neural network (CNN) is employed, making use of their combined strengths to address effectively the nonlinear relationship between wheel polygonization order, amplitude, and the dynamic response of the axle box. Simultaneously, the feature fusion method is adopted to analyze both time-domain and frequency-domain features holistically, facilitating the precise identification of wheel polygonization.

3.3. Wheel polygonization identification framework

The method proposed in this paper for identifying wheel polygonization order and its corresponding level encompasses several stages: wheel OOR and ABA data collection from field tests, numerical modeling and verification, ABA data pre-processing using ADSA (described below), feature extraction, and training using CNN. Subsequently, the method is verified using measured data, also obtained from field tests. The entire workflow of the identification process is illustrated in Fig. 7.

4. Wheel polygonization identification method

4.1. Establishment and validation of the vehicle-track coupled dynamic model

The rail transit system is a complex nonlinear multi-body dynamic system, comprising the car body, bogie frame, wheelsets, vehicle suspensions, and track system. A three-dimensional dynamic model, incorporating the coupling of the vehicle and track dynamics, is established using SIMPACK [49] as shown in Fig. 8. A metro vehicle is studied in this paper using the parameters listed in Table 1 for the vehicle-track coupled system, taking into account of the flexibilities of both the wheelset and the track. The track model represents a slab track, where the rail flexibility is neglected to enhance the computational efficiency. However, it includes the rail mass and the fasteners, which were represented in the model by stiffness and viscous damping elements as listed in Table 1. The model is utilized to generate a large number of samples for use in the Convolutional Neural Network (CNN) for a broader range of scenarios beyond the limitations of available measured data. Using a dynamic vehicle-track coupled model allows the generation of a large and diverse dataset that covers various conditions and track configurations that can be used for both training and validation of the CNN.

Research findings [50] have highlighted the substantial influence of rail fastener stiffness on the ABA, thereby affecting the identification outcomes. To widen the scope of the simulation model, two different values of fastener stiffnesses (soft and stiff) in the vertical direction are considered. The train speed was set to 70 km/h. A large number of simulations are carried out using this model using the excitations of different track irregularities and wheel OORs, generating a substantial number of data samples in the time-domain for the ABA. The two rail pad stiffness values are applied in the model. To check the realism of the model, the simulation results are compared with measured ones from the field tests, as shown in Fig. 9 in the form of the power spectral density (PSD) of the ABA. In these simulations, the wheel OOR data obtained from the direct measurements together with a representative track irregularity is employed as the excitation for the dynamic simulation. The influence of the possible failure of components such as bearings is not considered in this paper.

The P2 resonance can be seen as the broad peak at around 40 Hz in Fig. 9(a) and around 60–70 Hz in Fig. 9(b). These differences in P2 frequency are an important reason why the identification method should take account of differences in track properties. The calculated ABA results show a good agreement with the measurements, thus demonstrating the validity of the vehicle-track coupled dynamic model. This gives confidence to use samples of ABA data generated from the model in the proposed method.

4.2. Sample database

4.2.1. Data collection of OORs and ABAs

Based on the vehicle-track coupled dynamic model established in the previous section, the simulation models are configured under conditions encompassing two different values of fastener stiffness and two sets of diverse track irregularities. The vertical stiffness of the two fasteners is set as 20 MN/m and 80 MN/m. The two groups of track irregularities are based on the AAR class 5 spectrum [51] and a modified track irregularity spectrum, as shown in Fig. 10. The distinctive feature of the track irregularity spectrum is that it is characterized by a relatively high amplitude of the long-wave components and a comparatively low amplitude of the short-wave ones. To enhance the diversity of the track irregularities considered, the modified track irregularity consists of a reduction in the excitation component of the long wavelength irregularity and an increase in the component of the short-wave irregularity. Measurements presented in [52] showed that the long-wavelength track irregularity spectrum of slab tracks is flatter and lower compared to conventional ballast tracks. These features give a spectrum that is more similar to the track irregularity spectra in the metro system under study.

To give the neural network model a higher applicability, it is necessary to ensure a diverse set of training samples are used. This allows the model to learn comprehensively the characteristics across various sample types. However, incorporating more complex and diverse sample sets also introduces higher training challenges and prolonged training durations. To address these considerations and maintain sample diversity, this study focuses on a specific type of metro vehicle, with the properties listed in Table 1. Two trains of this type were selected for the measurement study, and the wheel OOR was measured multiple times before and after re-profiling the wheels.

In this paper, a dataset encompassing 500 sets of measured wheel profiles, which exhibit various levels of wear, was gathered. (The dataset of wheel polygonization levels could also be generated randomly). The roughness amplitude of various polygonal orders

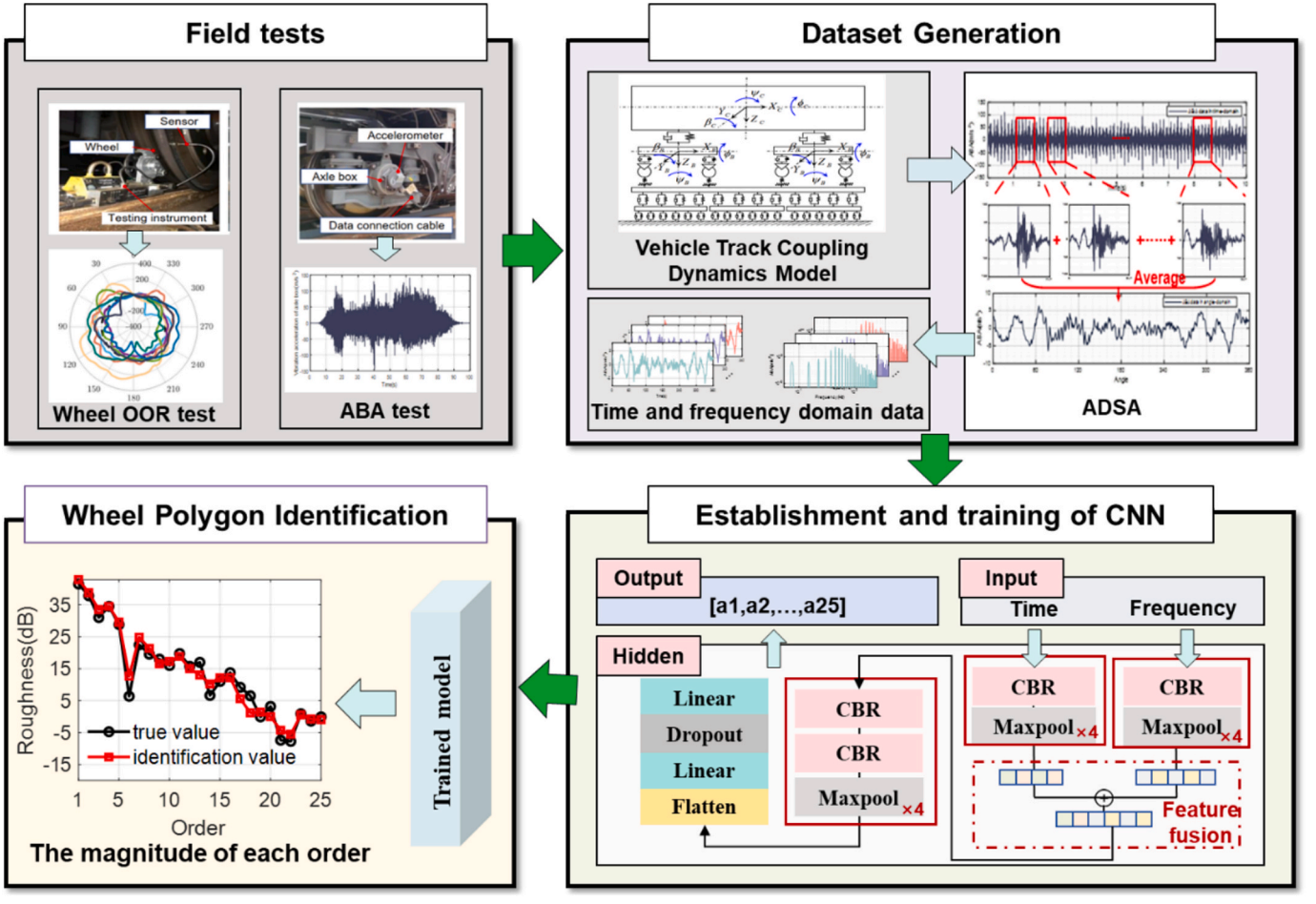

Fig. 7. Workflow of the wheel polygonization identification framework based on CNN regression model.

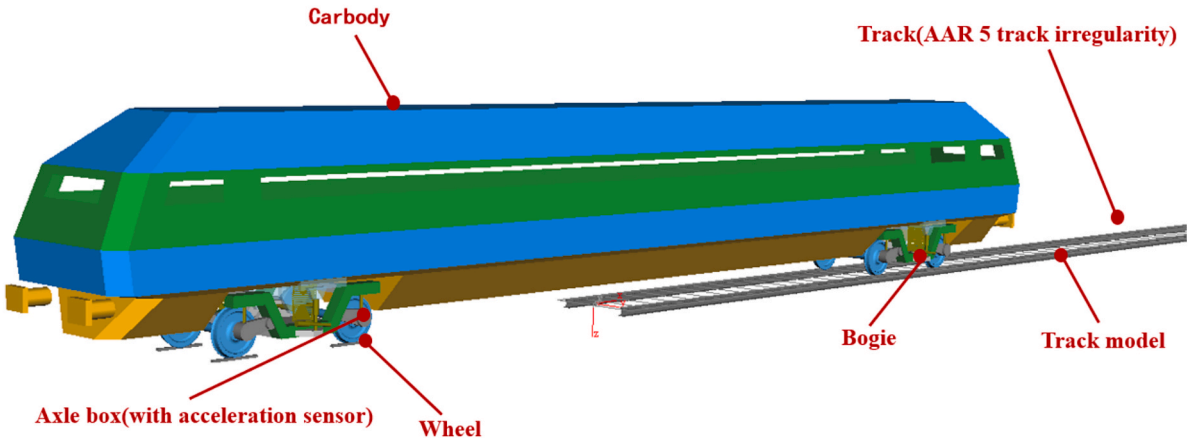

Fig. 8. The vehicle-track coupled dynamic model.

Table 1
Parameters of the vehicle–track coupled dynamic model.

Parameter	Value	Unit
Wheelset mass	1180	kg
Wheelset roll moment of inertia	636	$kg·m^2$
Wheelset pitch moment of inertia	85	$kg·m^2$
Wheelset yaw moment of inertia	636	$kg·m^2$
Bogie frame mass	2026	kg
Bogie frame roll moment of inertia	1225	$kg·m^2$
Bogie frame pitch moment of inertia	944	$kg·m^2$
Bogie frame yaw moment of inertia	2606	$kg·m^2$
Car body mass	23,124	kg
Car body roll moment of inertia	39,857	$kg·m^2$
Car body pitch moment of inertia	1,085,179	$kg·m^2$
Car body yaw moment of inertia	1,063,714	$kg·m^2$
Longitudinal stiffness of primary coil spring per axle box	0.7	MN/m
Lateral stiffness of primary coil spring per axle box	0.7	MN/m
Vertical stiffness of primary coil spring per axle box	0.911	MN/m
Vertical damping of primary hydraulic damper per axle box	15	kN·s/m
Longitudinal stiffness of air spring	0.17	MN/m
Lateral stiffness of air spring	0.17	MN/m
Vertical stiffness of air spring	0.3	MN/m
Vertical damping of secondary hydraulic damper	40	kN·s/m
Lateral damping of secondary hydraulic damper	55	kN·s/m
Rail mass per unit length	60	kg/m
Track gauge	1435	mm
Rail inclination	1:40	/
Vertical stiffness of rail fastener (soft)	20	MN/m
Vertical stiffness of rail fastener (stiff)	80	MN/m
Lateral stiffness of rail fastener	30	MN/m
Vertical damping coefficient of rail fastener	10	kN.s/m
Lateral damping coefficient of rail fastener	15	kN.s/m

between the 1st and the 25th are shown in Fig. 11(a) for examples of these measured wheel profiles. The abscissa in the figure denotes the wheel polygonal orders, while the ordinate represents the roughness rms amplitude at each order expressed in decibels. There is a very wide range of amplitudes of each order for these 500 different wheel profiles. The polygonal wear of different wheels can be very different due to various reasons, such as operational mileage, reprofiling method, traction/braking torques and so on. Thus, it is necessary but difficult to measure the polygonization levels of all wheels regularly and accurately.

To quantify the degree of dispersion in the wheel OOR data, the standard deviation of amplitudes of different orders was determined from the 500 measured profiles. The results are presented in Fig. 11(b), from which it can be observed that there is a large standard deviation for all orders, with an average value of 10.5 dB. This confirms that the 500 collected data samples exhibit significant diversity, providing a greater variety of data for the CNN and enhancing its applicability. With the samples of wheel circumferential profile acquired from the test used as the excitation, the vibration responses of the vehicle system in operation are

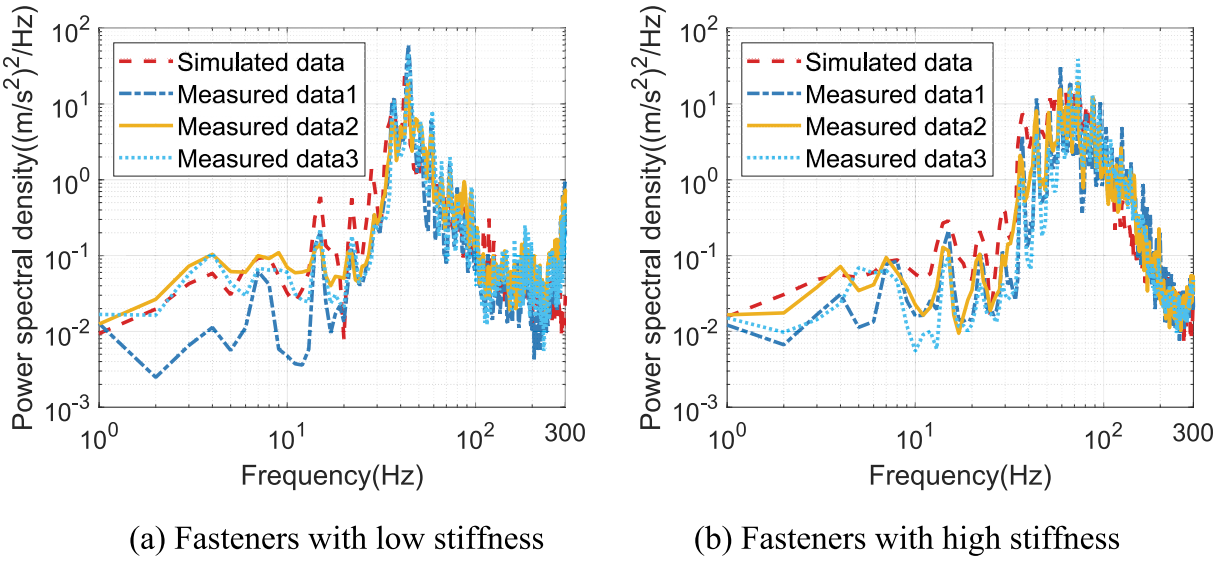

Fig. 9. Comparison between PSD of calculated and measured ABA for two values of fastener stiffness.

calculated with the dynamic model. Utilizing the Design of Experiments (DOE) function in SIMPACK, the 500 wheel OOR excitations combined with the four working conditions (two different track irregularities and two values of fastener stiffness) are processed in batches, generating a total of 2000 ABA data samples as responses. Each data segment has a length of 10 s and a sampling frequency of 5120 Hz. As explained above, these 2000 data sample sets exhibit rich diversity and complexity, ensuring that the neural network trained with this dataset has greater applicability. However, it also entails increased challenges and time consumption during the training phase.

4.2.2. *Pre-processing of ABA data with ADSA*

The measured ABA data acquired from the tests are recorded as discrete time series with a sampling rate of 5120 Hz. They encapsulate the total vibration response of the axle box due to the influence of both wheel and track excitations, along with other external factors. Therefore, it is imperative to preprocess the data to minimize the impact of track irregularities and rail roughness, aiming to retain and isolate information solely related to wheel polygonization.

The angular-domain synchronous averaging (ADSA) method, commonly used in fault diagnosis of rotating machinery [53–55], is adept at extracting periodic signal components from composite signals. Unlike other sources of excitation (which are often temporary and only present on specific track sections), wheel polygonization exhibits a consistent periodic characteristic throughout the entire train operation. ADSA was employed for its advances in removing non-periodic noise from signals, making it highly suitable for rotational periodic problems such as wheel polygonization. Therefore, preprocessing raw data with ADSA achieves a critical improvement in OOR identification accuracy by reducing the noise introduced by these other factors.

The fundamental principle involves resampling the original time-domain signal within the angular period of the periodic signal from the rotating structure. This conversion transforms the time-domain signal into an angular-domain signal, facilitating analysis of the periodic signal. Making use of the inherent periodic characteristics of each wheel polygonization order, the ADSA method effectively separates the excitation signal caused by wheel OOR from the complex vibration signal. This process results in the extraction of the signal with high correlation to wheel OOR for subsequent data processing. Based on this, a novel angular-domain averaging method is proposed, which relies on synchronously measured speed data. When the speed fluctuates, the acceleration signal of the axle box can be precisely divided into multiple segments, each corresponding to the wheel rotation period. It is assumed that the rotation speed is constant during one revolution, or only varies slowly. These segments are subsequently superimposed and averaged to enhance signal clarity.

The flow chart of the ADSA method used here is shown in Fig. 12. It can effectively separate ABA signals generated due to the wheel OOR from those due to track irregularity or rail roughness excitations even where the speed may vary. This is explained in more detail in the following.

It can be assumed that the collected ABA signal $x(t)$ is the superposition of the periodic signal $w(t)$ and the non-periodic signal $n(t)$, namely:

$$x(t) = w(t) + n(t) \tag{5}$$

where t represents time, $w(t)$ is a periodic signal related to the wheel polygonization, and $n(t)$ is an aperiodic signal not related to the wheel polygonization, which is due to other excitations and may be considered as noise.

Then it is necessary to extract the signal $w(t)$ related to the wheel polygonization from the ABA signal $x(t)$. Since $w(t)$ is assumed to

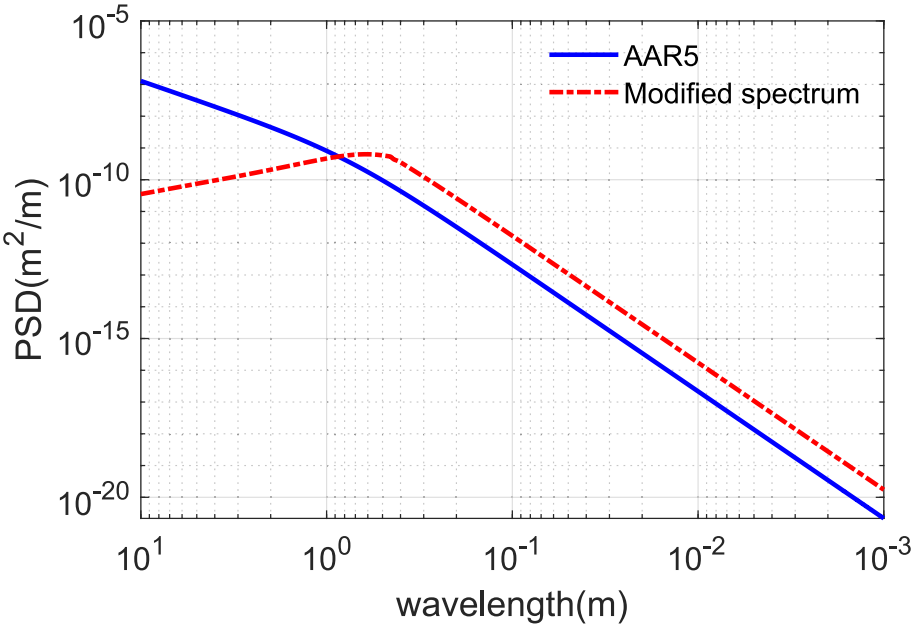

Fig. 10. AAR5 and modified track irregularity.

be periodic with a period of the wheel rotation,

$$w(t) = w(t+kT), k = 1, 2, \cdots \tag{6}$$

where t represents time, T represents the wheel rotation period, and k is the index of the k-th wheel rotation period. Subsequently, the ABA signal $x(t)$ can be partitioned according to the wheel rotation period T to derive the ABA for each wheel rotation cycle.

In the case of a vehicle undergoing speed changes, the signal is not exactly periodic in time and a straightforward division from the time-domain signal is not feasible. To overcome this, the relationship between speed and distance is utilized. The acceleration signal is resampled to correspond to an average speed, and the resulting signal is treated as a periodic one.

In this context, $x(t)$ is divided into P segments, each corresponding to one revolution of the wheel. Concurrently, the time domain signal is converted into an angle-dependent signal. The signal of the i-th segment, denoted as $x(\theta_i)$, is expressed as follows:

$$x(\theta_i) = w(\theta_i) + n(\theta_i) \tag{7}$$

where θ_i represents the i-th segment angular domain signal, $w(\theta_i)$ represents the signal component in the angular domain signal related to the wheel out-of-roundness, $n(\theta_i)$ represents the signal component not related to the wheel polygonization in the angular domain signal.

Finally, the P signal segments are averaged to obtain the output signal y, and due to the incoherence of non-periodic signals [56], the following relation is obtained:

$$y = \frac{1}{P}\sum_{i=1}^{P} x(\theta_i) \approx w(\theta_i) + \frac{1}{\sqrt{P}} \cdot n(\theta_i) \tag{8}$$

Because the wheel OOR signal is periodic, it remains unchanged after averaging, while the other non-periodic signals are weakened by a factor of $\sqrt{P}$ after averaging. When P is large enough, the other signals that are regarded as noise are sufficiently reduced. Here, P is set to be 160. Thus, the wheel polygonization signal can be separated from the other signals. The output signal y can approximately represent the angular-domain signal of ABA caused only by the wheel OOR within one rotation period. The preprocessed data is then Fourier transformed to obtain the frequency domain spectrum, as shown in Fig. 13.

As shown in the figure, compared with the original signal the noise information in the signal that is unrelated to the wheel polygonization is greatly attenuated after applying the ADSA pre-processing, while the information related to the wheel polygonization is preserved. The signal that remains is dominated by frequency components at the various orders of wheel polygonization.

4.2.3. Establishment of sample database

The sample database required by the neural network consists of ABA data in both the time domain and the frequency domain. First, the time-domain data sample set is established after pre-processing the raw ABA data from each model simulation with ADSA as described above. Second, the data sample set in the frequency domain is obtained by applying a Fourier transform to the above time-domain data. Finally, 80 % of the sample set, that is, data from 1600 model simulations, are selected as the training set for training the

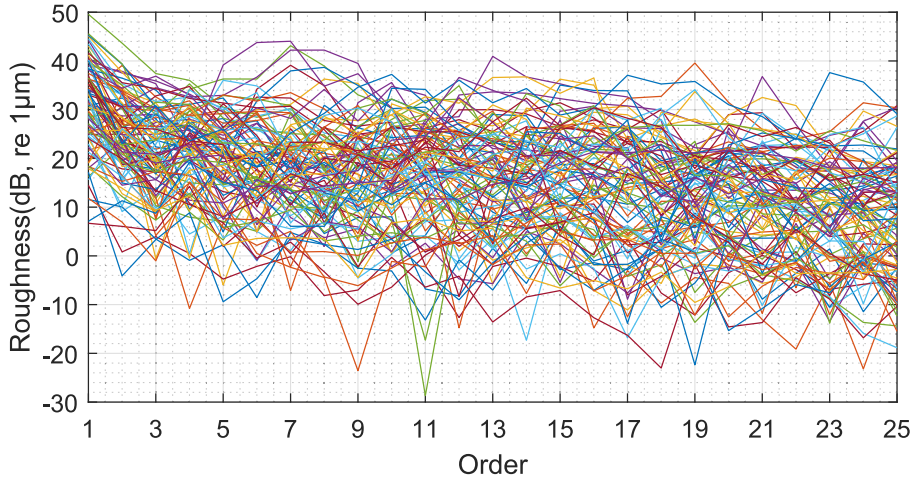

(a) Wheel roughness level

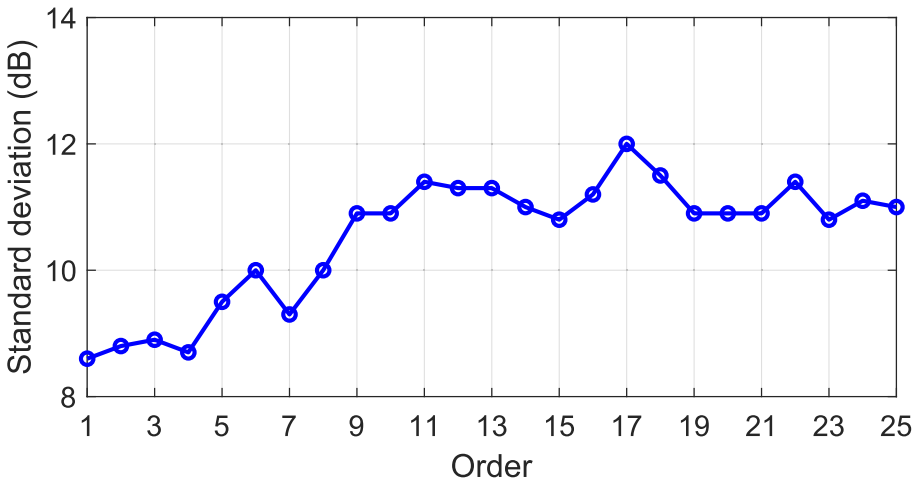

(b) Standard deviation

Fig. 11. 100 examples of measured level and standard deviation of each order of wheel polygonization.

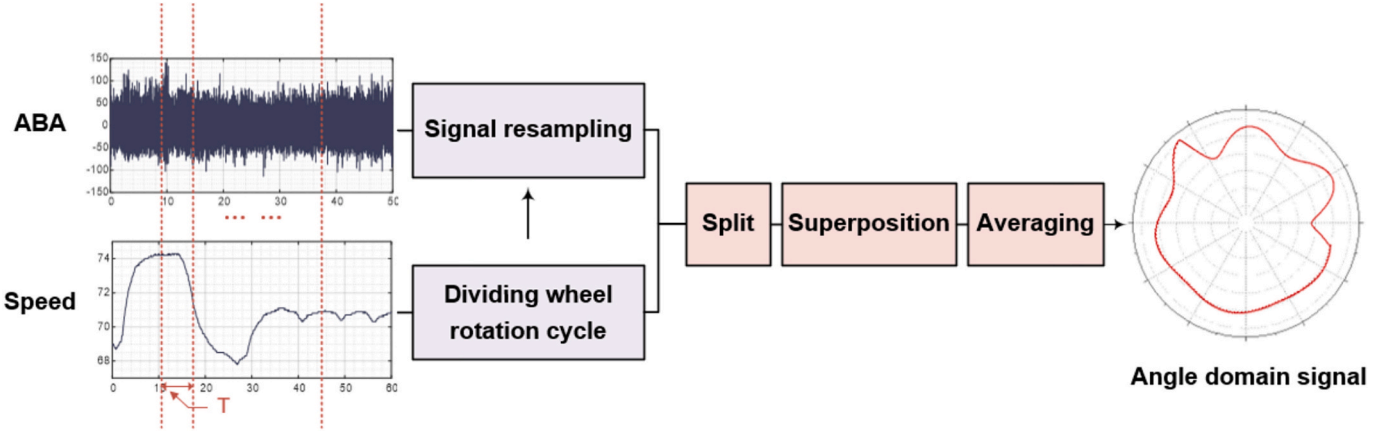

Fig. 12. Flow chart of data pre-processing based on ADSA.

neural network model, and data from the remaining 400 simulations are used together with the measured dataset as the test set for checking the accuracy of the identification method.

4.3. Setup and training of CNN

Considering the time-domain and frequency-domain characteristics of the acceleration of the axle box, a convolutional neural network model based on feature fusion was constructed based on the one-dimensional CNN combined with regression analysis. The neural network model mainly includes two parts. The first part is used to extract the feature vectors in the time domain and the frequency domain. The second part is used to extract features from the coupled vectors after feature fusion, and this is combined with the regression analysis to obtain the amplitude of each order of the wheel polygonization.

The feature vectors are extracted in the time domain and the frequency domain. For time-domain signal processing, the Deep Convolutional Neural Networks with Wide First-layer Kernel (WDCNN) model [57] is adopted. Its structural feature is that the first layer is a large convolution kernel of size 64×1, and the subsequent convolution layers are all small convolution kernels of size 3×1. The convolution kernel in the first layer is large, so that it can reduce redundant information, filter noise pollution, and extract relevant features of wheel polygonization from large scales. The remaining 3×1 three-layer convolution kernel can extract the order and amplitude relationship of the wheel polygonization from a deeper level. For signal processing in the frequency domain, unlike the time-domain signals, if the first-layer large convolution kernel method is adopted, the frequency resolution will increase. Therefore, in the frequency-domain signal processing, the first three layers adopt a small convolution kernel with a size of 3×1, while the last layer adopts a convolution kernel with a size of 5×1. After the feature vector is extracted, the time-domain and frequency-domain feature vectors are spliced and fused to obtain the coupled signal. For coupled signal processing, a feature extraction model of two layers of convolution plus one layer of pooling is adopted; that is, a pooling layer is placed after every two CBR modules to extract features, and the convolution kernels adopt a kernel size of 3×1, a total of four layers of convolutional networks. The structure for the CNN for this method is shown in Fig. 14. The parameters for each layer in the model are chosen as shown in Table 2.

The Mean-Square Error (MSE) is selected as the loss function, which is calculated as the mean square error obtained by each training step between the forward propagation prediction result and the real value used as input. The MSE is calculated [58] as follows

$$MSE = \frac{1}{n}\sum_{i=1}^{n}(y_i - \hat{y}_i)^2 \tag{9}$$

where y represents the actual value of the i-th data point, and y_i represents the predicted value of the i-th data point. Here, the unit of MSE is dB^2. The closer the MSE value is to 0, the better the prediction accuracy of the model is.

The Adam optimization algorithm [59] is applied to calculate the gradient of the loss function with respect to each parameter, and the weight parameters w of the neural network are updated iteratively through back-propagation, which could improve the training effect. The test set samples are input into the established CNN regression model for iterative training. If the loss function of the test set no longer decreases, the training will stop. The learning rate, a crucial hyperparameter in both supervised learning and deep learning, plays a decisive role in determining the convergence of the loss function to the local minimum and the speed at which such

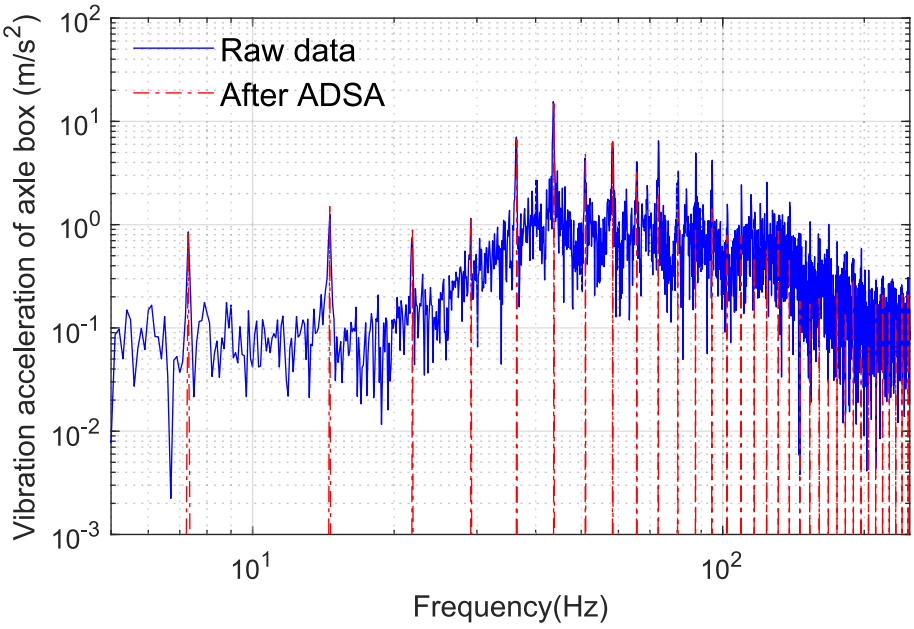

Fig. 13. Comparison of ABA signal in the frequency domain before and after pre-processing with ADSA method.

convergence occurs. Here, a learning rate of 0.001 is employed along with a batch size of 256 samples.

An example illustrating the changes in the MSE during the training process is presented in Fig. 15. The plot reveals a continuous decrease in the MSE as the number of training iterations increases, signifying an improvement in the training effectiveness. By the 102nd training iteration, the MSE reached its optimal value at 7.39 dB^2, corresponding to a Root Mean Squared Error (RMSE) of 2.7 dB.

5. Verification and discussion

A method of using the axle box acceleration signal to identify the amplitude of each order of the wheel polygonization has been proposed, as described above. Its main steps can be summarized as follows: (1) The ADSA method is applied to preprocess the ABAs of the sample set, which can reduce the noise of the ABA response from other factors except for wheel OOR; (2) The feature fusion and neural network regression analysis methods are combined and then a large amount of data training is carried out; (3) The neural network model is used to identify the level of each order of the wheel polygonization from ABA. These steps have been carried out using simulated data based on measured wheel OOR and track unevenness data using the dynamic model that has been verified in Section 4.

To evaluate the accuracy of the identification method, in this section it is applied to measured data. Comparisons are also made with results obtained using some alternative approaches. To illustrate the applicability of the proposed method, the measured ABA signals of vehicles running in different situations are selected for analysis.

5.1. *Verification and comparison between different methods*

To illustrate the effectiveness of the proposed wheel polygonization identification method based on the angular domain combined with the neural network, a comparison is made here between the identification results obtained by this full ADSA-CNN method, results obtained from CNN alone, and those from a simplified method based on the integration of acceleration combined with the ADSA method; in each case results are compared with the directly measured OOR results. The basis of this final method is that the circumferential displacement profile of the wheel can be approximated by applying a double integration to the acceleration of the axle box. This should give a good approximation to the wheel OOR at frequencies well below the P2 resonance frequency. This double integration can also be performed in the frequency domain.

The measured acceleration signals of the axle boxes obtained from the different wheels of the two trains are chosen before wheel re-profiling, and the above three methods are used to identify the wheel roughness. The results for two wheels from each of two trains are

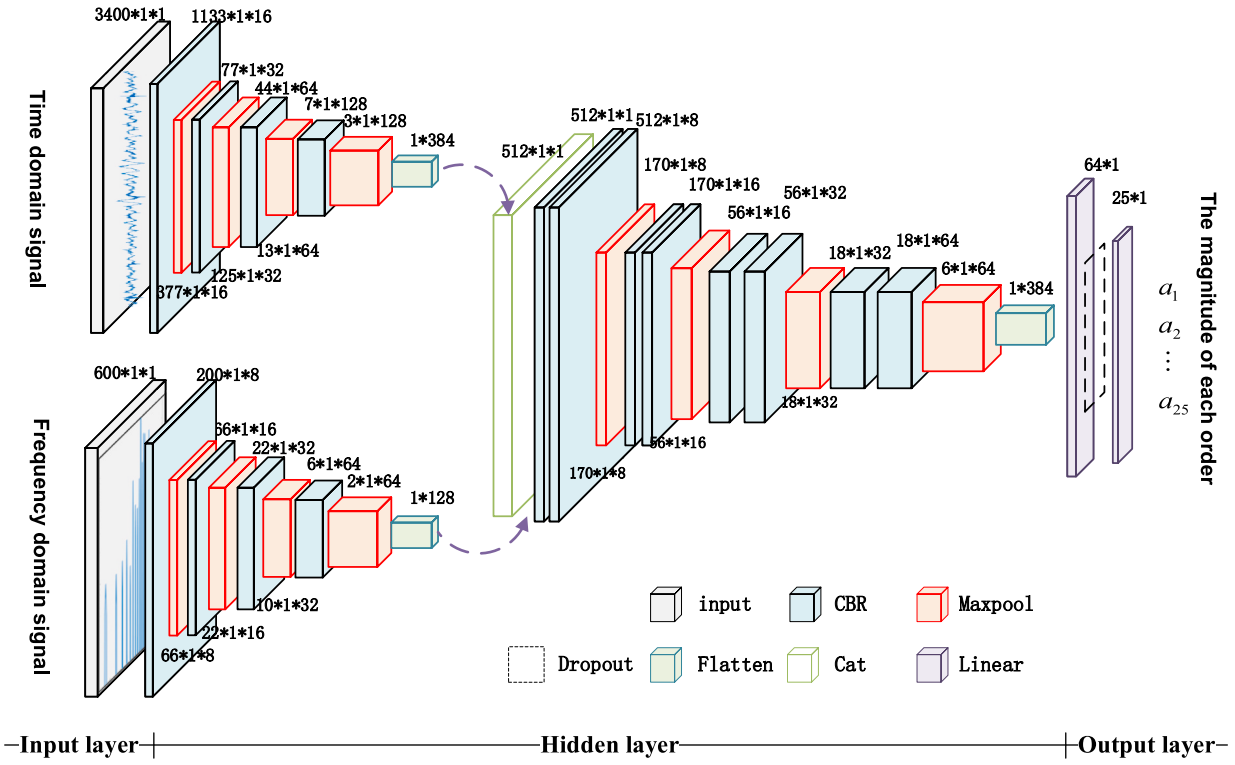

Fig. 14. Structure diagram of CNN for wheel polygonization identification.

Table 2
Parameters of CNN structure.

	Layers	Kernel size	Stride	Number of kernels	Padding
Networks for extracting time domain features	Convolutional Layer1	64 × 1	3	16	0
	Pooling Layer1	3 × 1	3	16	/
	Convolutional Layer2	3 × 1	1	32	1
	Pooling Layer2	3 × 1	3	32	/
	Convolutional Layer3	3 × 1	3	64	0
	Pooling Layer3	3 × 1	3	64	/
	Convolutional Layer4	3 × 1	2	128	1
	Pooling Layer4	2 × 1	2	128	/
Networks for extracting frequency domain features	ConvolutionalLayer1	3 × 1	3	8	0
	Pooling Layer1	3 × 1	3	8	/
	Convolutional Layer2	3 × 1	1	16	1
	Pooling Layer2	3 × 1	3	16	/
	Convolutional Layer3	3 × 1	1	32	1
	Pooling Layer3	3 × 1	3	32	/
	Convolutional Layer4	5 × 1	1	64	0
	Pooling Layer4	3 × 1	3	64	/
Networks for extracting coupled vector features	Convolutional Layer1	3 × 1	1	8	1
	Convolutional Layer2	3 × 1	1	8	1
	Pooling Layer1	3 × 1	3	8	/
	Convolutional Layer3	3 × 1	1	16	1
	Convolutional Layer4	3 × 1	1	16	1
	Pooling Layer2	3 × 1	2	16	/
	Convolutional Layer5	3 × 1	1	32	1
	Convolutional Layer6	3 × 1	1	32	1
	Pooling Layer3	3 × 1	2	32	/
	Convolutional Layer7	3 × 1	1	64	1
	Convolutional Layer8	3 × 1	1	64	1
	Pooling Layer4	3 × 1	3	64	/

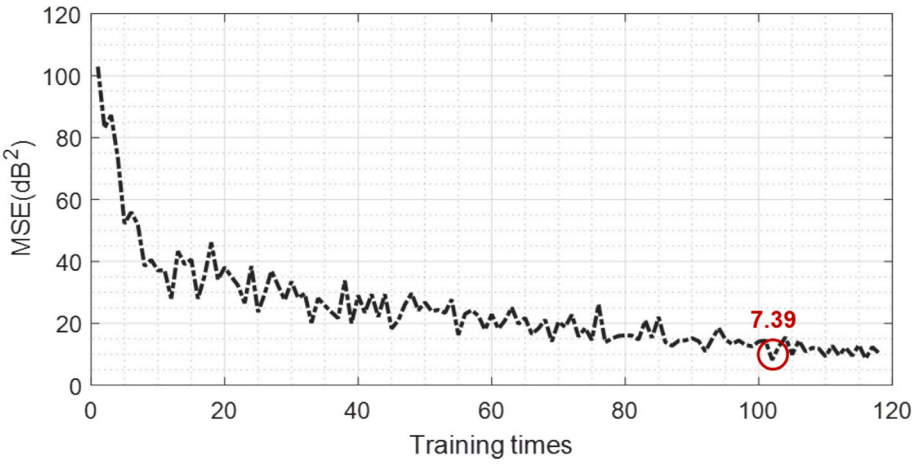

Fig. 15. The change of MSE with training times.

shown in one-third octave bands in Fig. 16 and compared with the ISO 3095:2013 limit curve [60]. This limit curve is intended as a threshold for the rail roughness applying in measurements of new rail vehicles, but it can also be seen as an indication of good practice.

It can be seen from the results that the wheel roughness in each wavelength band before wheel re-profiling seriously exceeds the limit curve from ISO 3095:2013, which will have an important impact on ride comfort, noise and structural fatigue. At the same time, although the three methods achieve good identification of wheel OOR, the method of ADSA-CNN gives the best agreement with the measured values. To quantify and compare the overall accuracy of the three methods, the root mean square error (RMSE) of the roughness levels in dB at wheel OOR orders 1–25 is determined. The results are shown in Table 3.

Among the three methods used for wheel polygonization detection, the ADSA-CNN method exhibits the smallest RMSE, suggesting that this method combines the advantages of the other two methods. It utilizes the angular-domain synchronous averaging method to extract relevant components more related to the wheel OOR and utilizes the ability of CNN to solve non-linear problems to determine the magnitude of each order accurately in the presence of different track stiffnesses and vehicle speeds.

To illustrate further the accuracy of the three methods for the detection of each order of polygonization, the relative errors of the

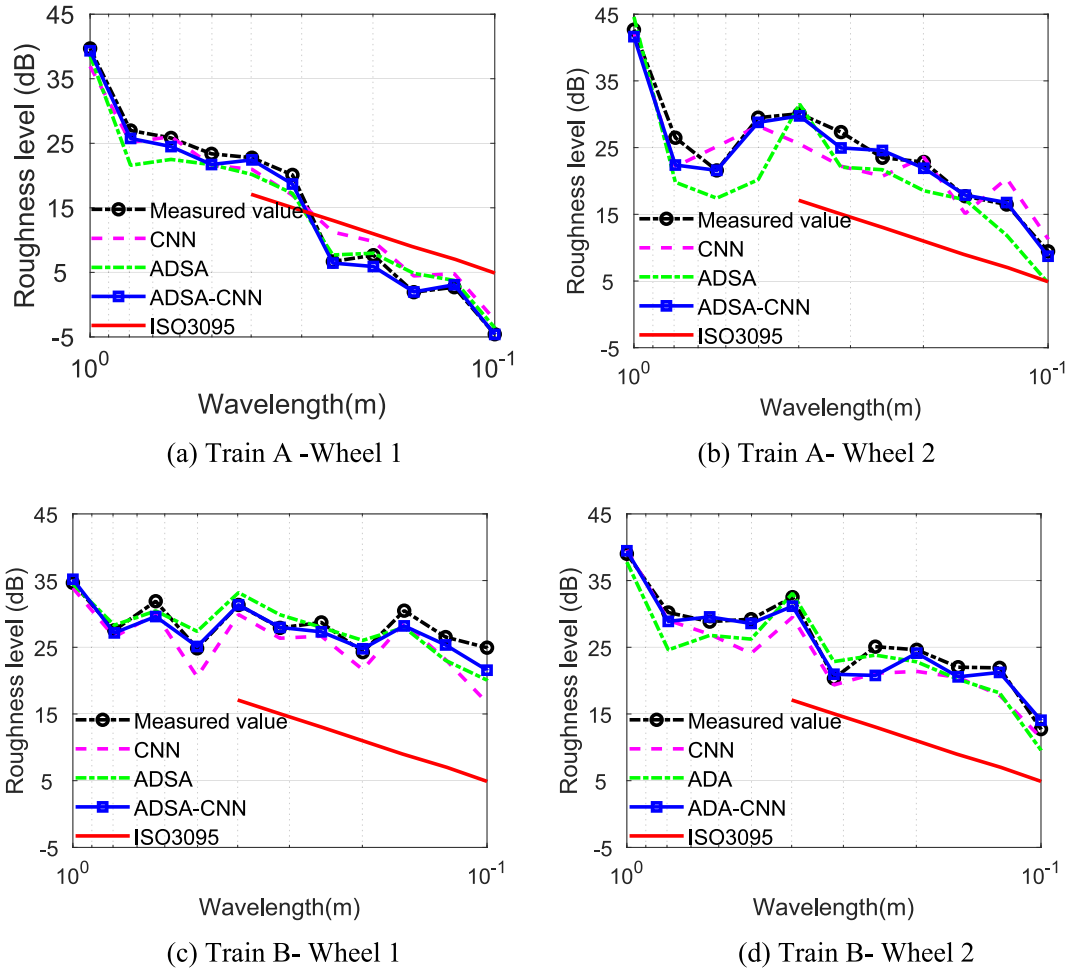

(a) Train A -Wheel 1

(b) Train A- Wheel 2

(c) Train B- Wheel 1

(d) Train B- Wheel 2

Fig. 16. Identification results of different methods before wheel re-profiling.

Table 3
Comparison of the RMSE values between the three methods (Unit: dB).

		ADSA	CNN	ADSA-CNN
Train A	Wheel 1	3.5	4.8	2.4
	Wheel 2	5.1	3.5	1.7
Train B	Wheel 1	3.2	4.2	1.9
	Wheel 2	3.5	4.0	2.2
Average		3.8	4.1	2.0

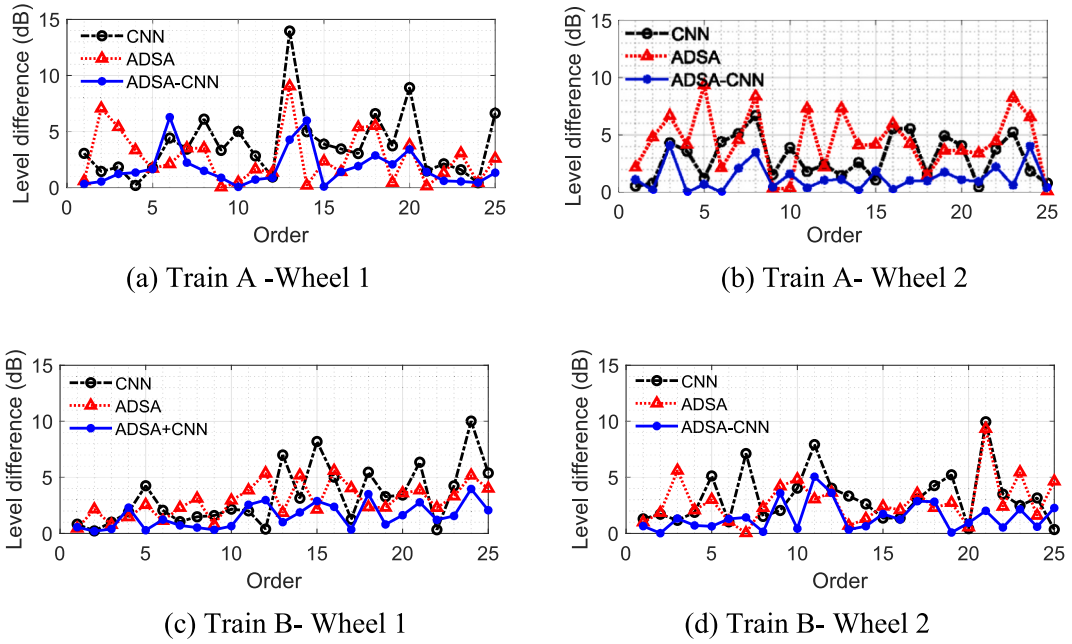

Fig. 17. Comparison of absolute values of relative errors between the three methods before wheel re-profiling.

wheel roughness at each order identified by the three methods are shown in Fig. 17 as level differences. The relative error is the difference between the identified level of wheel polygonization with the respective method and the measured result for each order. Fig. 17 shows that the difference between the identification values and the actual values with the ADSA-CNN method is on average around 1.5 dB, whereas for the CNN method it is around 3 ~ 4 dB, and for the ADSA method it is around 3 dB. The level differences for the ADSA and CNN methods have significant fluctuations, with some orders exhibiting larger errors. However, the ADSA-CNN method shows a good performance in identifying most orders, with recognition errors generally below 5 dB. This indicates a more stable and accurate identification for the various wheels from different trains. Compared with the results from references [27] and [33], the errors or RMSE values in the current results are lower. Additionally, it was noted [27] that the methods proposed in recent studies were more effective for the quantitative detection of dominant wheel orders rather than non-dominant or low order wheel polygonization.

5.2. The influence of different factors

5.2.1. The degrees of wheel polygonization

In the above, the identification of each wheel polygonization order was carried out on the wheels before re-profiling, and a relatively accurate result was obtained. However, due to the lower roughness level of the wheels after re-profiling, the noise in the acceleration signal of the axle box is relatively large, which often brings difficulties for the identification. In order to verify the identification effect of this method on the wheels with low levels of OOR, the ADSA-CNN method is adopted to identify the wheel roughness from the wheel OOR and vibration measurements carried out after wheel reprofiling. The identification results of four wheels are shown in Fig. 18 in one-third octave bands.

The OOR levels of the two wheels from Train A are now below the ISO 3095 limit curve after reprofiling. The roughness of the wheels from Train B also decreased, although the wheels are not exceptionally smooth, and the roughness levels at different wavelengths still exceed the standard. The relative errors of the first 25 orders of the wheel OOR after re-profiling are shown in Fig. 19. It can be seen from Fig. 19 that the proposed ADSA-CNN method also gives a reliable identification of the wheel roughness after re-profiling.

The RMSE values of the two groups of data are listed in Table 4. This confirms that the proposed method also has a good identification accuracy after wheel re-profiling, although the RMSE values after wheel re-profiling are larger than those before re-profiling.

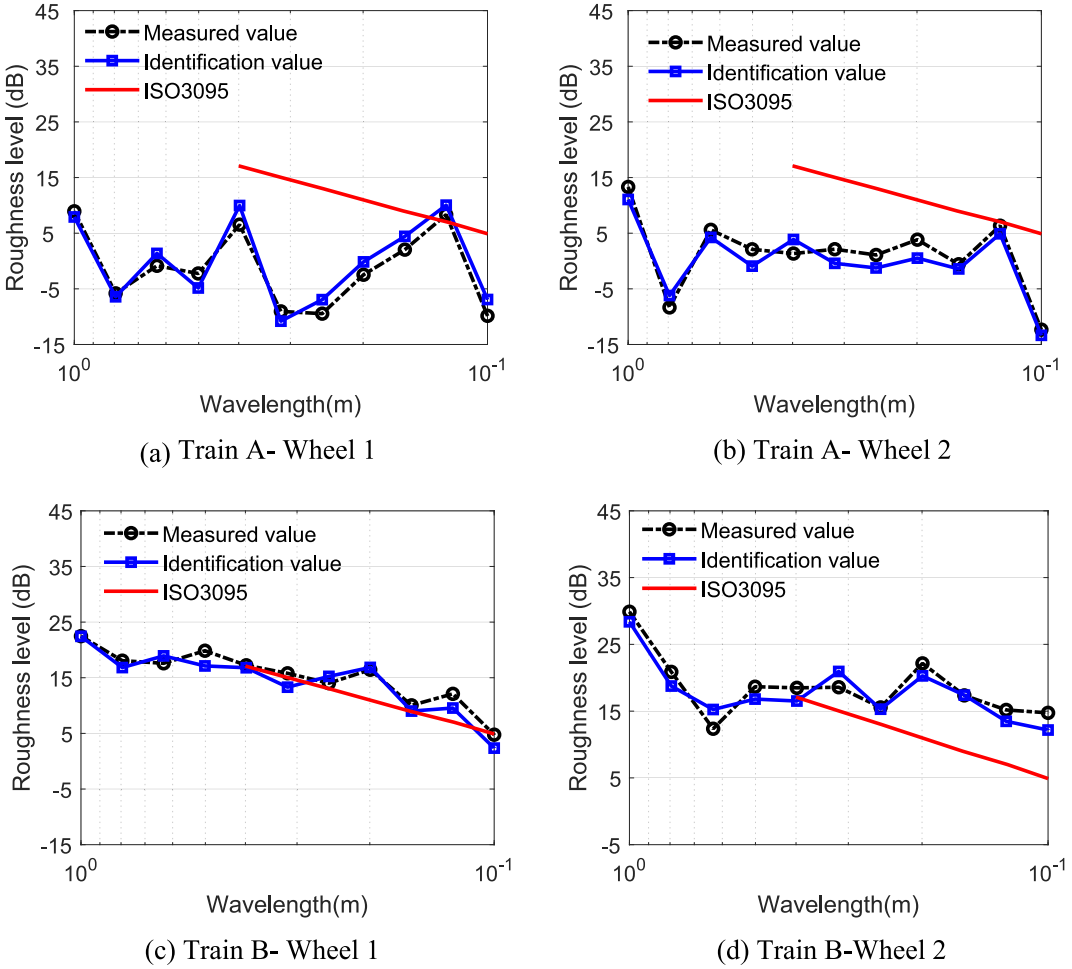

Fig. 18. Comparison of identified results after wheel re-profiling.

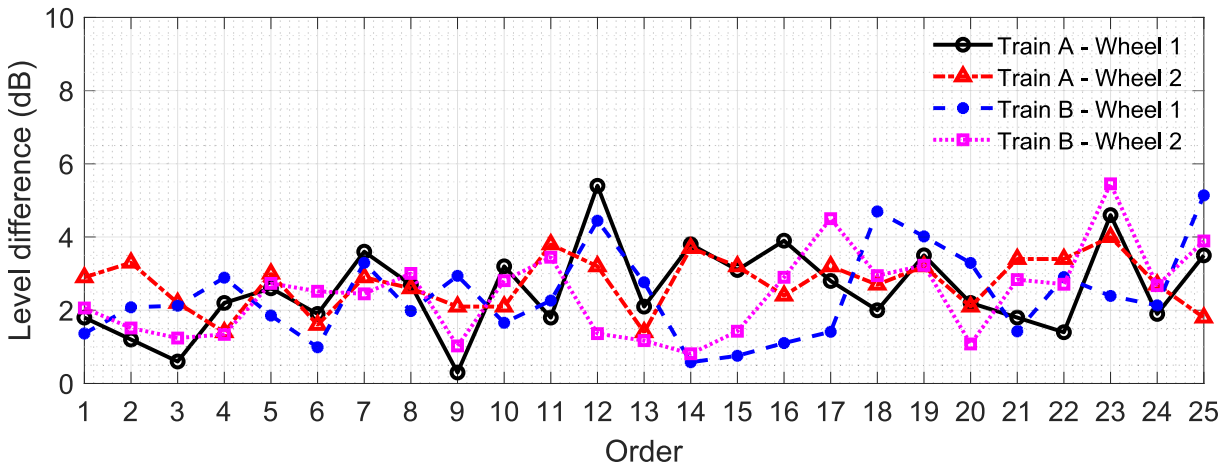

Fig. 19. Identification relative error of each order of the wheels after re-profiling.

As indicated in the tabular data, the ADSA-CNN method gives commendable accuracy even for wheels with low levels of OOR after undergoing wheel reprofiling operations. This suggests that the method described in this study demonstrates a good applicability across different degrees of wheel polygonal wear. However, on average, the relative error is larger for wheels with small OOR, for

Table 4
RMSE values after wheel re-profiling and before re-profiling (Unit: dB).

	Train A		Train B		Average
	Wheel 1	Wheel 2	Wheel 1	Wheel 2	
After re-profiling	2.8	2.8	2.7	2.7	2.8
Before re-profiling	2.4	1.7	1.9	2.2	2.0

which other factors, such as track irregularities, have a larger influence. The accuracy increases with the development of wheel polygonization, which is beneficial for on-board identification of wheel polygonization in the field.

5.2.2. Different track stiffness

From the measured ABA results in Fig. 4, it can be seen track stiffness typically affects the ABA response. To verify the effectiveness of the proposed method in identifying polygonization under different track conditions, ABA data from the vehicle running on different track locations with varying fastener stiffness were selected. The polygonization was identified based on the ADSA-CNN method, and the RMSE between the identified and measured levels was calculated. The identification results are presented in Fig. 20 for one wheel as an example.

It can be seen from Fig. 20 that this method gives a similar identification accuracy for the two fastener stiffnesses, with corresponding RMSE values of 2.5 dB for both high and low stiffness.

A comparison of identification results obtained using training datasets with one or two values of fastener stiffness is shown in Fig. 21. The results indicate that when the dataset includes samples from these two fastener stiffness conditions, this method effectively reduces the influence of differences in fastener stiffness on the results. Where greater variations in track properties are expected, a wider range of track properties could be included in the training data.

5.2.3. Speed fluctuation

To verify the influence of speed on the identification accuracy, the ABA signals corresponding to the vehicle running at relatively constant and variable speed conditions were selected for identifying the polygonization. The vehicle speed and corresponding ABA signals are shown in Fig. 22.

In the first case, the vehicle maintains a speed of around 71 km/h, whereas in the second case the speed fluctuated between 67 to 75 km/h. These speed fluctuations can cause variations in the ABA signal, thereby affecting the identification accuracy. The identification results for the two operating conditions are shown in Fig. 23. Good identification results were achieved under both operating conditions as shown in the figure. However, the identification result under constant speed condition is better than that under variable speed condition for most wheel polygonization orders.

The RMSE value under the constant speed condition (2.6 dB) was smaller than that under the variable speed condition (3.5 dB), indicating that the fluctuation in vehicle speed has a certain impact on the identification results. It should be noted that all training data were generated from the numerical model at a constant speed of 70 km/h. If the running speed is close to this value, the identification accuracy can be high. To improve the accuracy for other speeds, the training data could be extended to include a variety of speeds. However, in practice the trains on a metro network often run at a consistent constant speed.

5.3. Comparison with different preprocessing and machine learning methods

5.3.1. Preprocessing methods

ADSA offers clear advantages as a preprocessing method for rotationally periodic problems. Its key strength lies in operating directly in the angular domain, aligning signals with the rotational dynamics of the wheel to accurately capture periodic features. In contrast, methods like EMD (Empirical Mode Decomposition) and EEMD (Ensemble Empirical Mode Decomposition), while effective for handling non-stationary signals by decomposing them into intrinsic mode functions (IMFs), are sensitive to noise, prone to mode mixing, and computationally intensive. Although EEMD improves upon EMD by incorporating Gaussian white noise (GWN) to enhance signal separation, it still lacks the rotational synchronization inherent in ADSA, making it less effective for isolating periodic defects like wheel polygonization. ADSA also handles variations in train speed effectively, as rotational features are inherently tied to the angular domain, making it well-suited for railway applications. Moreover, it is computationally efficient and integrates well with deep learning models.

As for the GWN method, it introduces high-frequency components into acceleration signals, helping the diagnostic network resist high-frequency impacts [34]. While it improves robustness to noise by diversifying the data and reducing overfitting, its white noise amplitude must be determined empirically through multiple trials. However, GWN lacks the ability to directly amplify periodic characteristics associated with rotational defects, such as wheel polygonization, limiting its effectiveness in tasks that rely heavily on periodic feature extraction.

A comparative analysis of these preprocessing methods, shown in Fig. 24 for one example wheel, demonstrates that ADSA outperforms the other approaches in terms of the overall RMSE across all 25 orders. In each case the same CNN is applied after the preprocessing has been carried out. ADSA effectively isolates periodic components of wheel polygonization while suppressing non-periodic noise, ensuring greater clarity and amplification of periodic features. This makes it particularly robust against noise and speed variations, making it well-suited for rotational periodicity analysis. Additionally, ADSA is significantly more computationally

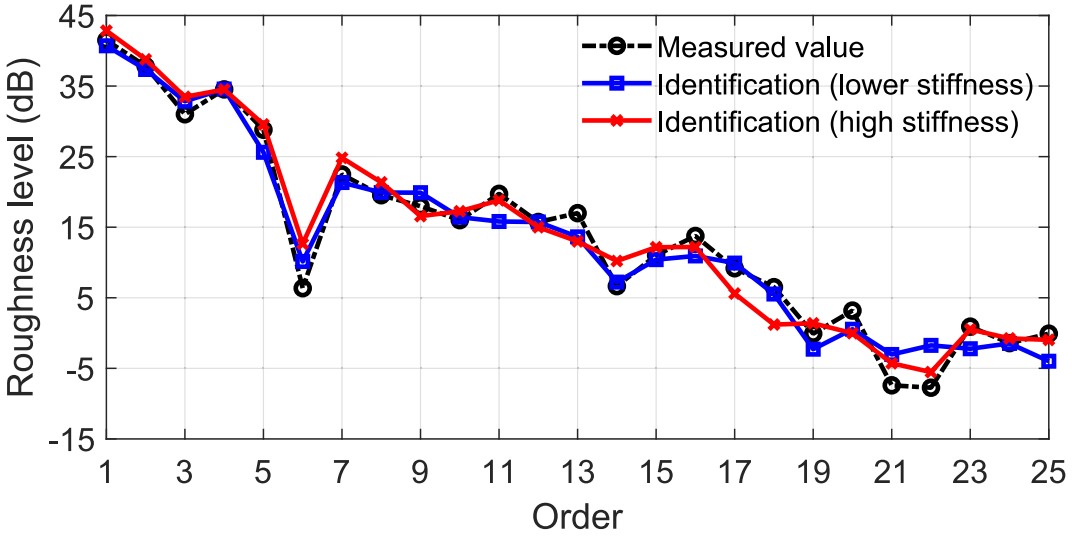

Fig. 20. Comparison of wheel polygonization identified results with different fastener stiffness.

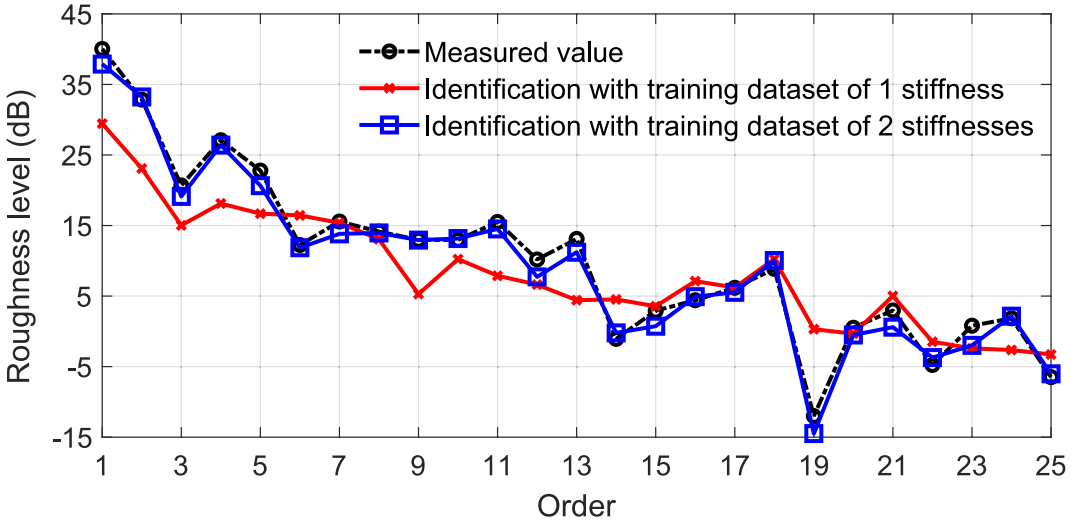

Fig. 21. Comparison of results identified using training datasets based on different fastener stiffness values.

efficient than EMD or EEMD, further enhancing its practicality.

5.3.2. Machine learning models

To demonstrate the effectiveness of the proposed method, commonly used machine learning models, including the OORNet model [33] and the CNN-LSTM model[34], were compared for their identification performance on the same example wheel. The neural network architectures for the proposed method and OORNet[33] are similar, except that the latter incorporates an additional time–frequency diagram. By contrast [34] employs the most complicated network architecture with only one frequency domain data feature. Consequently, the training rounds and time are both significantly higher for the models in [33] and [34]. Besides, an alternative model, ADSA-SVM (support vector machine)[61] has been included. While SVM offers a simpler and more computationally efficient workflow, it lacks the hierarchical feature extraction capabilities of the deep learning models. The features of these approaches are summarized in Table 5.

All the identification results at orders up to the 25th obtained with the different methods are shown in Fig. 25. The identification effect is best for the proposed method ADSA-CNN in this manuscript and GWN-OORNet[33] also has a good performance. The CNN-LSTM model from [34] is more complicated, yet due to its costly calculation, the training rounds may not be enough to get a better result here. It gives a similar result with OORNet, although better than the SVM model.

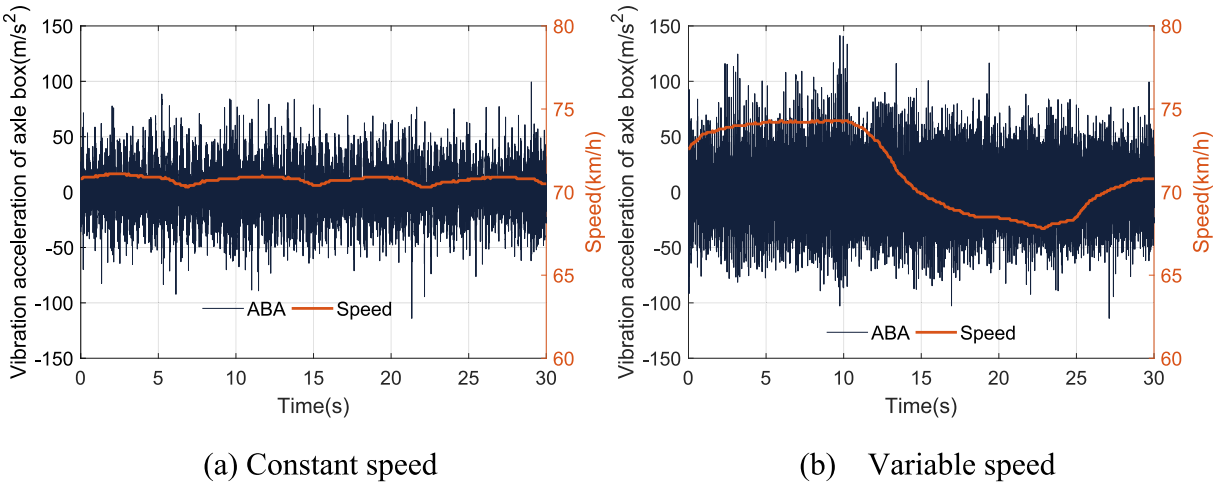

Fig. 22. ABA signals under constant and variable speed conditions.

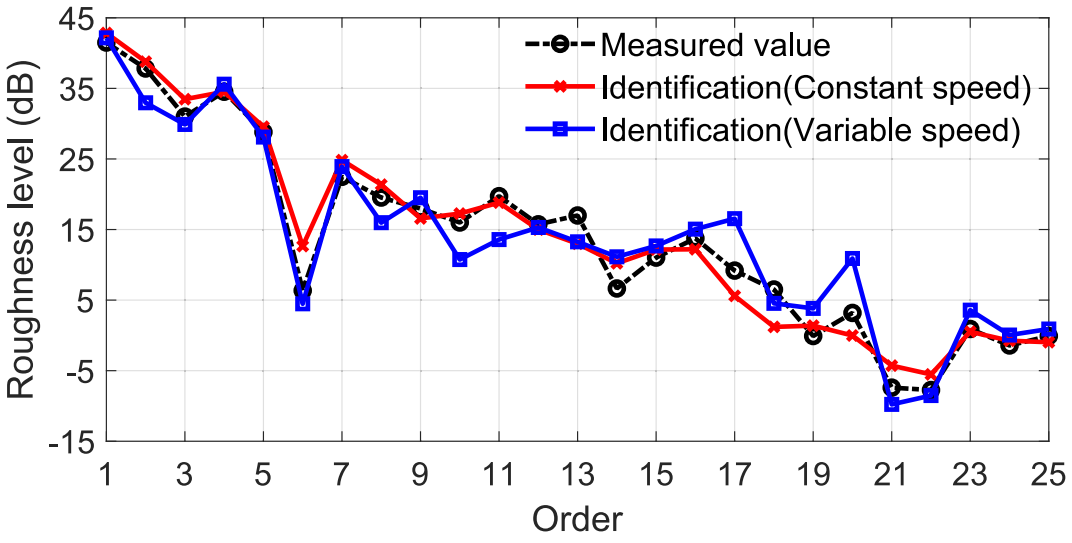

Fig. 23. Comparison of identified results under constant and variable speed conditions.

6. Conclusions

A method is proposed for identifying wheel polygonization levels with different orders, based on a combination of CNN and ADSA methods. A validated coupled vehicle-track dynamic model with varying track fastener stiffnesses is established to generate a large number of ABA signals under different conditions. Based on this, a dataset of 2000 samples is created for CNN training and verification. The ADSA method is applied to preprocess the data, reducing the noise from track roughness. A CNN model, incorporating feature fusion techniques, is developed to identify wheel polygonization based on the temporal and spectral characteristics of the axle box acceleration signals. Combining the CNN and regression analysis, the amplitude of each wheel polygonization order can be deduced from the ABA signals. After extensive training, the model achieves an overall average RMSE of 2.7 dB for identifying the levels of the 1st to 25th orders of wheel polygonization, significantly outperforming methods based on only CNN or ADSA. Higher orders of wheel polygonization could be identified with the proposed framework and method, provided that rail flexibility is incorporated into the model. However, this inclusion would significantly increase computation time.

The superiority and applicability of the proposed ADSA-CNN method were also discussed. The mean RMSE values for the three methods in identifying the wheel polygonization before reprofiling were approximately 2.0 dB (ADSA-CNN), 4.7 dB (ADSA) and 4.1 dB (CNN) respectively, from which is evident that the ADSA-CNN method outperforms the other two methods. Then the influence of different factors, including wheel polygonization severity, different track fastener stiffness, and variable vehicle speed, on the identification accuracy was analyzed. The results show that the severity of the wheel polygonization has an influence on the identification but the OOR after reprofiling could still be determined with reasonable accuracy (RMSE value after reprofiling: 2.8 dB, before

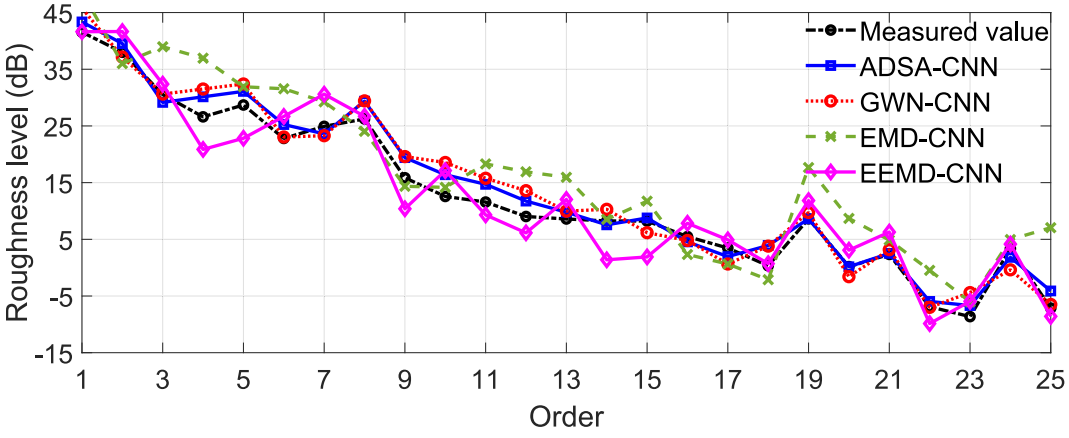

(a) Wheel polygonization level

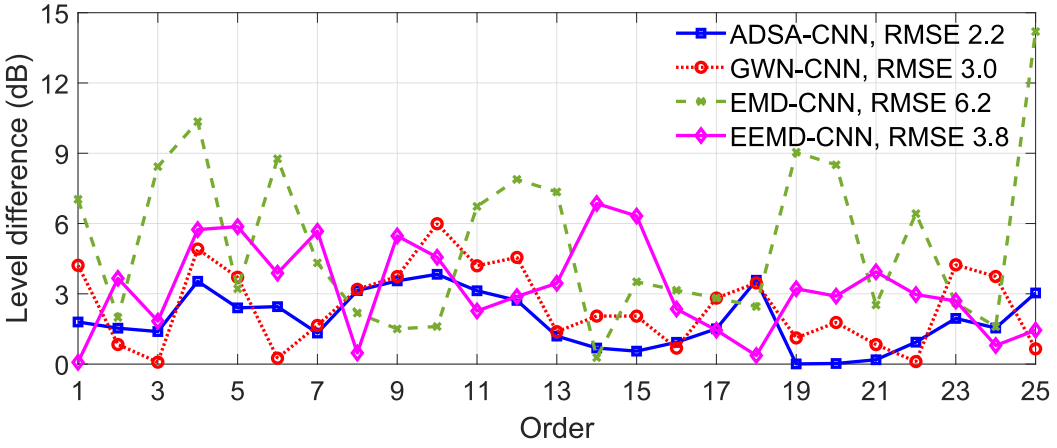

(b) Level difference

Fig. 24. The comparison of identification results between different pre-processing methods.

Table 5
Comparison between different machine learning models.

Parameter	The proposed method	OORNet [33]	CNN-LSTM [34]	SVM[61]
Data features	Time-domain, frequency-domain	Time-domain, frequency-domain, time–frequency diagram	Frequency-domain	Frequency-domain
Neural network	Two convolutions, concatenation, followed by one convolution	Three convolutions, concatenation, followed by one convolution	One convolution followed by 2 LSTM cells, concatenation	Kernel mapping layer (using RBF) – regression layer
Training rounds	100	500	75/150	/
RMSE	2.2	2.6	4.5/2.6	5.4

reprofiling: 2.0 dB). The ADSA-CNN method effectively mitigates errors caused by different track fastener stiffness, with a similar average RMSE value obtained under different stiffness conditions. This is achieved because the sample data was generated from the dynamic model with two widely different values of fastener stiffness. For more general applicability a wider range of track properties could be included in the training data in the future. Furthermore, the reliability of the OOR identification is affected by speed fluctuations (RMSE value: 2.6 dB with constant speed, 3.5 dB with speed fluctuation). It is therefore recommended to use data measured at a constant speed to improve the accuracy. Nevertheless, to widen the applicability the training data could be extended to include other speeds.

The proposed ADSA-CNN method has demonstrated clear effectiveness and advantages over various preprocessing techniques and

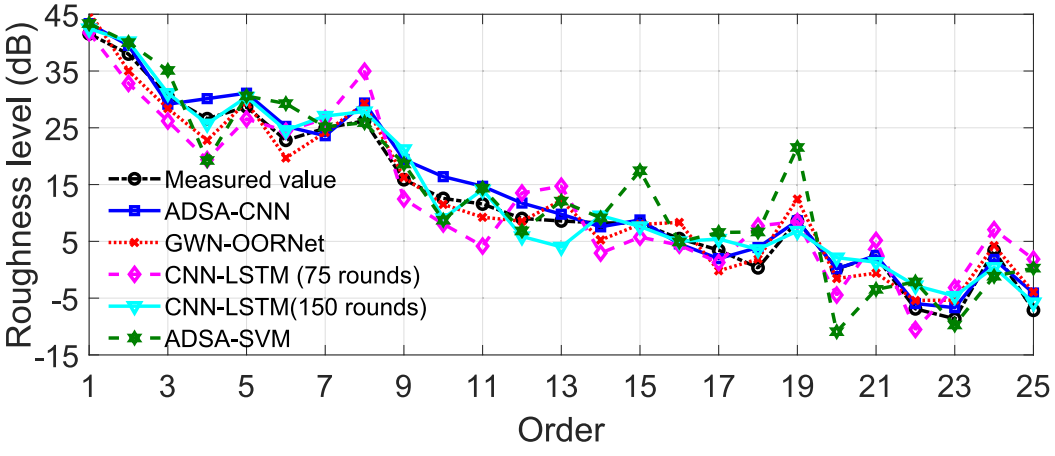

(a) Wheel polygonization level

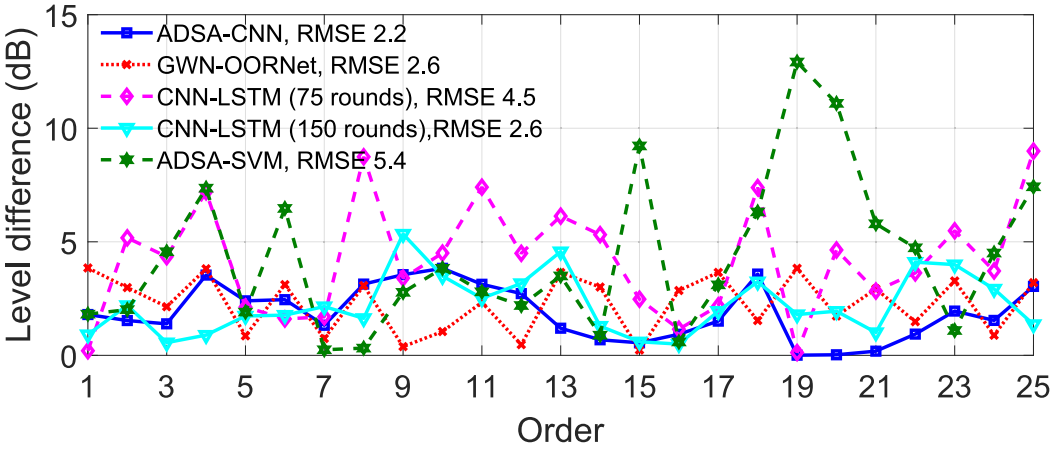

(b) Level difference

Fig. 25. Comparison of identification results obtained using different deep learning models.

machine learning models from the literature. While other approaches based on time–frequency analysis or advanced models exist, their suitability for this specific application requires evaluation. The ADSA-CNN method achieves high accuracy and computational efficiency in identifying wheel polygonization levels across different metro vehicles. ADSA excels at handling periodic rotational signals, while the CNN effectively captures critical features from the dataset. Additionally, the inclusion of a diverse training dataset incorporating metro trains and track stiffness variations ensures practical applicability. These elements collectively make the proposed method a robust and efficient solution for detecting metro wheel polygonization.

CRediT authorship contribution statement

Wenjing Sun: Writing – review & editing, Supervision, Resources, Project administration, Methodology, Investigation, Funding acquisition, Formal analysis, Conceptualization. **Xuan Geng:** Writing – original draft, Software, Methodology, Investigation, Formal analysis. **David J. Thompson:** Writing – review & editing, Validation, Supervision. **Tengfei Wang:** Investigation, Data curation. **Jinsong Zhou:** Resources. **Jin Zhang:** Investigation.

Declaration of competing interest

The authors declare that they have no known competing financial interests or personal relationships that could have appeared to influence the work reported in this paper.

Acknowledgements

This work was supported by the National Natural Science Foundation of China (Grant No. 52302477, 12304524).

Data availability

Data will be made available through the University of Southampton online repository.

References

[1] S. Iwnicki, J.C.O. Nielsen, G.Q. Tao, Out-of-round railway wheels and polygonization, Veh. Syst. Dyn. 61 (2023) 1787–1830.
[2] X.S. Jin, L. Wu, J.Y. Fang, S.Q. Zhong, L. Ling, An investigation into the mechanism of the polygonal wear of metro train wheels and its effect on the dynamic behaviour of a wheel/rail system, Veh. Syst. Dyn. 50 (2012) 1817–1834.
[3] P. Liu, S. Yang S, Y. Liu, Full-scale test and numerical simulation of wheelset-gear box vibration excited by wheel polygon wear and track irregularity, Mech. Syst. Signal Process. 167 (2022) 108515.
[4] W. Chen, H. Dai, R. Luo, Influence of high-order polygonal wheel on the dynamic performance of high-speed train, Journal of Railway Vehicles 52 (2014) 4–8, in Chinese.
[5] G.Q. Tao, M.Q. Liu, Q.L. Xie, Z.F. Wen, Wheel-rail dynamic interaction caused by wheel out-of-roundness and its transmission between wheelsets, Proc. Inst. Mech. Eng. f. J. Rail Rapid Transit 236 (2022) 247–261.
[6] J. Zhang, G. Han, X.B. Xiao, R.Q. Wang, Y. Zhao, X.S. Jin, Influence of wheel polygonal wear on interior noise of high-speed trains, J. Zhejiang Univ. Sci. 15 (2014) 1002–1018.
[7] R. Bogacz, K. Frischmuth, On dynamic effects of wheel-rail interaction in the case of Polygonalisation, Mech. Syst. Signal Process. 79 (2016) 166–173.
[8] T.F. Wang, J.S. Zhou, W.J. Sun, D. Thompson, Z. Zhang, Q. Wang, Fatigue analysis of coil springs in the primary suspension of a railway vehicle based on synthetic spectrum for time-varying vibration load, Proc. Inst. Mech. Eng. f. J. Rail Rapid Transit 237 (2023) 1164–1175.
[9] Z.W. Wang, P. Allen, G.M. Mei, R.C. Wang, Z.H. Yin, W.H. Zhang, Influence of wheel-polygonal wear on the dynamic forces within the axle-box bearing of a high-speed train, Veh. Syst. Dyn. 58 (2020) 1385–1406.
[10] L. Zhang, Z.W. Wang, Q. Wang, J.L. Mo, J. Feng, K.Y. Wang, The effect of wheel polygonal wear on temperature and vibration characteristics of a high-speed train braking system, Mech. Syst. Signal Process. 186 (2023) 109864.
[11] Y. Yu, L. Guo, H. Gao, A study on the effect of wheel-polygonal wear on dynamic vibration characteristics of urban rail vehicle axle-box bearings, Prognostics and Health Management Conference (PHM), IEEE (2023) 159–163.
[12] V. Belotti, F. Crenna, R.C. Michelini, G.B. Rossi, Wheel-flat diagnostic tool via wavelet transform, Mech. Syst. Signal Process. 20 (2006) 1953–1966.
[13] K. Bollas, D. Papasalousros, A. Anastasopoulos, Acoustic emission monitoring of wheel sets on moving trains, Constr. Build. Mater. 48 (2013) 1266–1272.
[14] J. Brizuela, C. Fritsch, A. Ibáñez, Railway wheel-flat detection and measurement by ultrasound, Transp. Res. C Emerg. Technol. 19 (2011) 975–984.
[15] Q. Sun, C. Chen, A.H. Kemp, P. Brooks, An on-board detection framework for polygon wear of railway wheel based on vibration acceleration of axle-box, Mech. Syst. Signal Process. 153 (2021) 107540.
[16] R.Q. Wang, Y. Li, L.X. Chu, Extraction method of significant polygons on railway vehicle wheels, Noise and Vibration, Control 37 (2017) 5–8, in Chinese.
[17] T. Staśkiewicz, B. Firlik, Out-of-round tram wheels–current state and measurements, Arch. Transp. 45 (2018) 83–93.
[18] Y. Song, L. Liang, Y.L. Du, B.C. Sun, Railway polygonized wheel detection based on numerical time-frequency analysis of axle-box acceleration, Appl. Sci. 10 (2020) 1613.
[19] W.T. Xu, M.R. Chi, W.B. Cai, G.Q. Tao, J.F. Sun, Y.B. Zhou, S.L. Liang, An anti-disturbance method for on-board detection of early wheel polygonal wear by weighted angle-synchronous moving average, Meas. 216 (2023) 112999.
[20] S.C. Yang, S.Y. Jang, E. Kim, Determination of upper limit of rail pad stiffness for ballasted and concrete track of high-speed railway considering running safety, J. Korean Soc. Railw. 14 (2011) 526–534, in Korean.
[21] X.W. Wu, M. Chi, Study on stress states of a wheelset axle due to a defective wheel, J. Mech. Sci. Technol. 30 (2016) 4845–4857.
[22] X.W. Wu, S. Rakheja, S. Qu, P.B. Wu, J. Zeng, A.K.W. Ahmed, Dynamic responses of a high-speed railway car due to wheel polygonalisation, Veh. Syst. Dyn. 56 (2018) 1817–1837.
[23] X.L. Wang, Research on the detection method of wheel roundness of urban rail train based on improved Wigner-Ville time-frequency analysis (Doctoral dissertation), Nanjing University of Science and Technology, Jiangsu, China, 2017 in Chinese.
[24] Z.J. Li, L. Wei, H.Y. Dai, J. Zeng, Recognition method of wheel flat based on Hilbert-Huang transform, J. Traffic Transp. Eng. 12 (2012) 33–41.
[25] P. Wang, X. Wang, Y. Wang, R.H. Zhang, Identification model of wheel out-of-roundness based on high-speed railway track unevenness, J. Southwest Jiaotong Univ. 55 (2020) 681–687, in Chinese.
[26] S.Q. Chen, K.Y. Wang, Z.W. Zhou, Y.F. Yang, Z.G. Chen, W.M. Zhai, Quantitative detection of locomotive wheel polygonization under non-stationary conditions by adaptive chirp mode decomposition, Railw Eng. Sci. 30 (2022) 129–147.
[27] Q.L. Xie, G.Q. Tao, S.M. Lo, W.B. Cai, Z.F. Wen, High-speed railway wheel polygon detection framework using improved frequency domain integration, Veh. Syst. Dyn. 62 (2024) 1424–1445.
[28] T.D. Carrigan, J.P. Talbot, Extracting information from axle-box acceleration: on the derivation of rail roughness spectra in the presence of wheel roughness, Noise Vib. Mitig. Rail. Transp. Syst. (2021) 286–294.
[29] T.D. Carrigan, J.P. Talbot, A new method to derive rail roughness from axle-box vibration accounting for track stiffness variations and wheel-to-wheel coupling, Mech. Syst. Signal Process. 192 (2023) 110232.
[30] D.C. Shi, Y.G. Ye, M. Gillwald, M. Hecht, Designing a lightweight 1D convolutional neural network with Bayesian optimization for wheel flat detection using carbody accelerations, Int. J. Rail Transp. 9 (2021) 311–341.
[31] L.X. Deng, Q.L. Xie, G.Q. Tao, Z.F. Wen, Identification method of wheel out-of-roundness state of high-speed train based on axle box vibration and dynamic model, J. Mech. Eng. 59 (2023) 110–121, in Chinese.
[32] B. Xie, S.Q. Chen, M.K. Xu, Y.F. Yang, K.Y. Wang, Polygonal Wear Identification of wheels based on optimized multiple kernel extreme learning machine, Chin. J. Theor. Appl. Mech. 54 (2022) 1797–1806, in Chinese.
[33] Y.G. Ye, B. Zhu, P. Huang, P. Peng, OORNet: A deep learning model for on-board condition monitoring and fault diagnosis of out-of-round wheels of high-speed trains, Meas. 199 (2022) 111268.
[34] M.Y. Dong, S.Q. Chen, B. Xie, K.Y. Wang, W.M. Zhai, A quantitative detection method for wheel polygonization of heavy-haul locomotives based on a hybrid deep learning model, Meas. 227 (2024) 114206.
[35] Q.S. Wang, Z.M. Xiao, J.S. Zhou, D. Gong, Z.G. Wang, Z.F. Zhang, T.F. Wang, Y.L. He, A new DFT-based dynamic detection framework for polygonal wear state of railway wheel, Veh. Syst. Dyn. 61 (2023) 2051–2073.
[36] Q.S. Wang, Z.M. Xiao, J.S. Zhou, D. Gong, Z.G. Wang, Z.F. Zhang, T.F. Wang, Y.L. He, A dynamic detection method for polygonal wear of railway wheel based on parametric power spectral estimation, Veh. Syst. Dyn. 61 (2023) 2352–2374.
[37] EN 15610:2019, Railway applications – Acoustics – Rail and wheel roughness measurement related to noise generation, European Committee for Standardization, Brussels, 2019.
[38] H. Fujiyoshi, T. Hirakawa, T. Yamashita, Deep learning-based image recognition for autonomous driving, IATSS Res. 43 (2019) 244–252.

[39] L. Wen, X.Y. Li, L. Gao, Y.Y. Zhang, A new convolutional neural network-based data-driven fault diagnosis method, IEEE Trans. Ind. Electron. 65 (2017) 5990–5998.
[40] S. Santurkar, D. Tsipras, A. Ilyas, A. Madry, How does batch normalization help optimization Adv, Neural Inf. Process. Syst. 31 (2018) 2483–2493.
[41] C. Gulcehre, M. Moczulski, M. Denil, Y. Bengio, Noisy activation functions, Proc. 33rd Int. Conf. Mach. Learn., 2016, pp. 3059-3068.
[42] F.Y. Zhou, L.P. Jin, J. Dong, A comprehensive review on convolutional neural networks, Chin. J. Comput. 40 (2017) 1229–1251, in Chinese.
[43] Y. L. Boureau, J. Ponce, Y. Cun, A theoretical analysis of feature pooling in visual recognition, Proc. 27th Int. Conf. Mach. Learn., 2010, pp. 111-118.
[44] Y. L. Boureau, N. L. Roux, F. Bach, J. Ponce, Y. LeCun. Ask the locals: multi-way local pooling for image recognition. Proc. 2011 Int. Conf. Comput. Vis., 2011, pp. 2651-2658.
[45] Q.J. Wang, X.H. Bao, Z. Qian, Nonlinear regression analysis based on genetic neural network, J. Hefei Univ. Technol. 28 (2005) 1053–1056, in Chinese.
[46] Q. Xu, Research on Methods for Nonlinear Regression Analysis (Master's thesis), Hefei University of Technology, 2009 (in Chinese).
[47] D.F. Specht, A general regression neural network, IEEE Trans. Neural Netw. 2 (1991) 568–576.
[48] D. Ramachandram, G.W. Taylor, Deep multimodal learning: a survey on recent advances and trends, IEEE Signal Process. Mag. 34 (2017) 96–108.
[49] Y. Ye, D. Shi, P. Krause, Q. Tian, M. Hecht, Wheel flat can cause or exacerbate wheel polygonization, Veh. Syst. Dyn. 58 (2020) 1575–1604.
[50] P. Wang, J.H. Xu, L. Wang, R. Chen, Effect of track stiffness on frequency response of vehicle-track coupled system, J. Railw. Eng. Soc. 31 (2014) 46–52, in Chinese.
[51] R.N. Iyengar, O.R. Jaiswal, Random field modeling of railway track irregularities, J. Transp. Eng. 121 (1995) 303–308.
[52] E. Ntotsios, D.J. Thompson, M.F. Hussein, A comparison of ground vibration due to ballasted and slab tracks, Transp. Geotech. 21 (2019) 100256.
[53] F. Bonnardot, M.E.I. Badaoui, R.B. Randall, J. Daniere, F. Guillet, Use of the acceleration signal of a gearbox in order to perform angular resampling with limited speed fluctuation, Mech. Syst. Signal Process. 19 (2005) 766–785.
[54] F. Combet, L. Gelman, An automated methodology for performing time synchronous averaging of a gearbox signal without speed sensor, Mech. Syst. Signal Process. 21 (2007) 2590–2606.
[55] H. Li, Y. Zhang, H. Zheng, Angle domain average and CWT for fault detection of gear crack, Fifth Int, Conf. Fuzzy Syst. Knowl. Discov., (2008) 137–141.
[56] B.Y. Song, Z. Jie, F. Zhang, Low-speed skewed gear fault diagnosis based on angle domain synchronous averaging and order analysis, J. Jilin Univ. 45 (2015) 454–459, in Chinese.
[57] W. Zhang, G.L. Peng, C.H. Li, Y.H. Chen, Z.J. Zhang, A new deep learning model for fault diagnosis with good anti-noise and domain adaptation ability on raw vibration signals, Sensors 17 (2017) 425.
[58] H. Zhao, O. Gallo, I. Frosio, J. Kautz, Loss functions for image restoration with neural networks, IEEE Trans. Comput. Imaging 3 (2017) 47–57.
[59] D.P. Kingma, J. Ba, Adam: A method for stochastic optimization, 3rd Int. Conf. Learning Representations, 2015.
[60] ISO 3095:2013: Acoustics - railway applications - measurement of noise emitted by railbound vehicles, International Organization for Standardization, Geneva, 2013.
[61] M.T. Xu, H.M. Yao, Fault diagnosis method of wheelset based on EEMD-MPE and support vector machine optimized by quantum-behaved particle swarm algorithm, Meas. 216 (2023) 112923.